Instabilities, Turbulence and Transport

Jiaqi Dong

Southwestern Institute of Physics, China
&
Institute for Fusion Theory and Simulation
Zhejiang University, China

2015 ITER International School
USTC, Hefei, China
December 14-18, 2015

Outline

1. Introduction
2. Instabilities
3. Turbulence and Zonal Flow
4. Transport
5. Summary

Outline

1. **Introduction**
2. **Instabilities**
3. **Turbulence and Zonal Flow**
4. **Transport**
5. **Summary**

- **Study of turbulence induced cross field transport in tokamak plasmas has made significant progress.**
- **The mechanism for such anomalous transport, in particular in pedestal, is still an open issue.**
- **Formation of large-scale structures such as zonal flows (ZFs) is universal in turbulent systems.**
- **Experimental identification of ZFs is important to understand transport and confinement in fusion plasmas.**
- **Basic methods and example results for the study of micro-instabilities, which may induce the anomalous transport, and turbulence and zonal flows are discussed.**

Outline

1. Introduction
2. **Instabilities**
3. Turbulence and Zonal Flow
4. Transport
5. Summary

(1) Instabilities in plasmas

MHD instabilities，micro-instabilities（induced by deviation from Maxwell distribution：Harris instability，loss corn instability, drift instability, trapped particle instability, micro-tearing instability etc.）

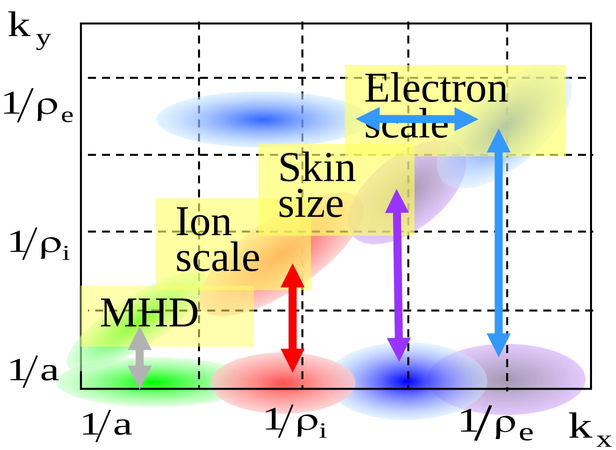

$a \sim 50cm$

$\rho_i \sim 2mm$

$\rho_e \sim 0.05mm$

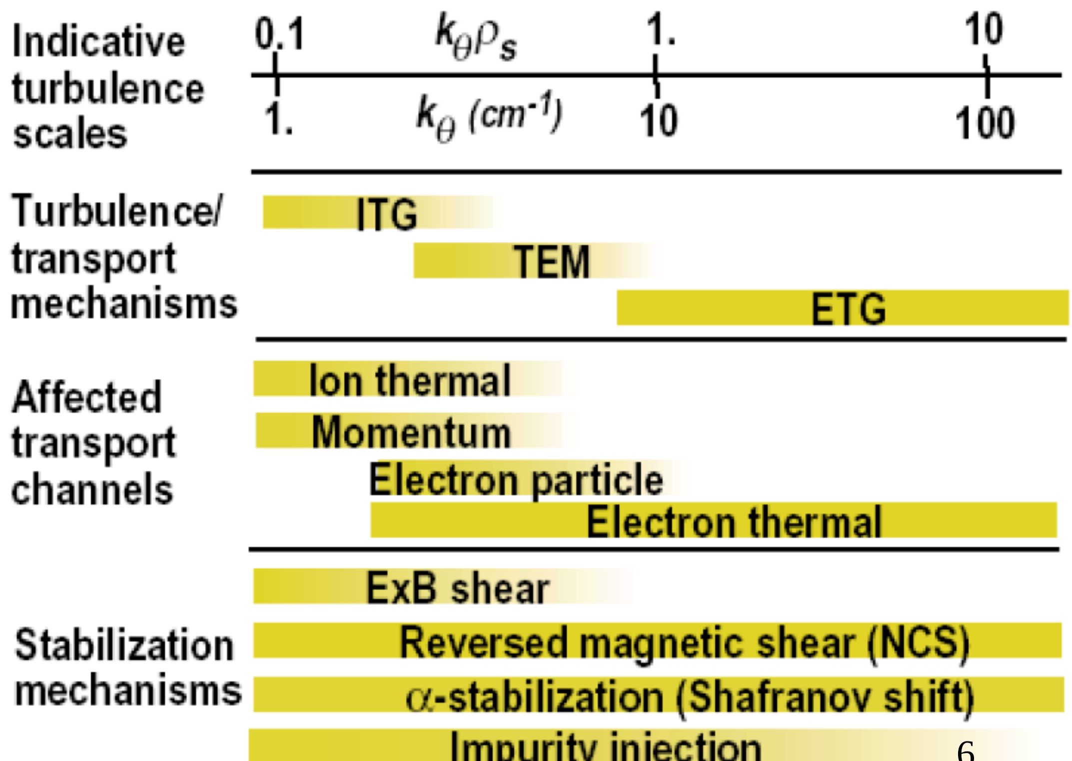

(2) Importance of micro-instability study

1)Explanation of direct experimental observations :

- **space plasma: satellite observation: φ, B**
- **fusion plasma: n, B, φ**

2)Looking for mechanisms of anomalous cross field transport

(particle, momentum and energy)

i)Classical transport:

$$\chi_e = 4.66\rho_e^2\upsilon_{ee}$$

$$\chi_i = 2\rho_i^2\upsilon_{ii}$$

TFTR results

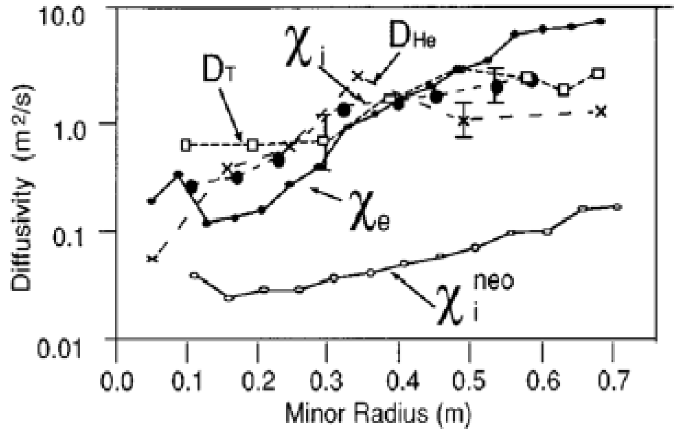

ii)Neoclassical transport

(banana regime)

$$\chi_e^{ne} \sim \varepsilon^{\frac{-3}{2}} q^2\rho_e^2\upsilon_{ee}$$

$$\chi_i^{ne} \sim \varepsilon^{\frac{-3}{2}} q^2\rho_i^2\upsilon_{ii}$$

$$\varepsilon = r/R$$

$$q > 1$$

iii)Turbulence induced (anomalous) transport

- Electric perturbations：

$$\delta v_\perp = \delta E_\perp / B,\ \Gamma = \langle \delta v_\perp \delta n \rangle, \quad q_j = \frac{3}{2} n_j \langle \delta v_\perp \delta T_j \rangle$$

- Magnetic perturbations：

$$\Gamma_j = \frac{n}{B} \langle \delta V_{\parallel j} \delta B_r \rangle$$

iv) Experimental observations

$$\chi_e^{\exp} \sim 100\, \chi_e^{ne}$$

$$\chi_i^{\exp} \sim 10\, \chi_i^{ne}$$

3）One of the major fields of magnetic fusion studies：

(i)Macro-instabilities； (ii)wave-particle interaction； (iii)micro-turbulence and anomalous transport； (iv)edge physics; (v)energetic particle physics。

(3)Roles of linear theory：saturation amplitude calculation needs inclusion of non-linear effects;

linear theory may：

(i) identify driving mechanisms；

(ii) identify criteria for instabilities；

(iii) identify thresholds of plasma density and temperature profiles (when turbulence induced transports dominate)；

(iv) benchmark non-linear codes

(v) provide estimate for transport; the characteristics of linear modes have relations with features of turbulences：

quasi-linear theory;

mixing length estimate： $\chi \sim \gamma / k^2$

Main driving mechanism --instabilities

Group	Instability	Source of free energy	Subspecies	Properties
Ion Instabilities	η_i modes	∇T_i	Slab modes Toroidal modes Trapped ion modes	$\omega \leq \omega_{*i}$ $\eta_i > \eta_{ic}$ $L_{T_i}/R < (L_{T_i}/R)_{crit}$
Electron instabilities	Electron Drift Waves	∇n_e	Slab modes Toroidal modes	$\omega \approx \omega_{*e}$
	Dissipative trapped electron modes	∇T_e		$\varepsilon\omega < \nu_e \leq \varepsilon^{3/2} V_{the}/qR$ $\varepsilon_n q < k_\perp \rho_s \leq \nu_e L_n/\varepsilon c_s$
	Collisionless trapped electron modes	∇T_e		$\nu_e < \varepsilon\omega \leq \varepsilon^{3/2} V_{the}/qR$ $\varepsilon_n q < k_\perp \rho_s \leq 1$
	η_e modes	∇T_e	Slab modes Toroidal modes	$\omega_{pe}/c < k_\perp < \rho_e^{-1}$ $k_\parallel V_{the}, \omega_{be} < \omega < \omega_{*e}$
	EM drift waves	∇n_e		$\omega \approx \omega_{*e}, k_\perp \rho_s \leq 1$
Fluid like instabilities	Resistive ballooning modes	∇P	Fast modes Slow modes	$\omega \approx \omega_{*e}$ $k_\parallel V_{the} < \omega$
	Current diffusive ballooning modes	∇P		$k_\parallel V_{the} < \omega$

(4)Fluid ion temperature gradient (ITG) mode

1) Basic equations:

Ion continuity equation:

$$\frac{\partial}{\partial t} n_i + \nabla \cdot (n_i \vec{v}_i) = 0 \qquad (1)$$

equation of motion of ions :

$$m_i n_i \left(\frac{\partial}{\partial t} + \vec{V}_i \cdot \nabla \right) \vec{V}_i = e n_i \left(\nabla \phi + \frac{\vec{V}_i \times \vec{B}}{c} \right) - \nabla P_i - \nabla \cdot \vec{\Pi}_i \qquad (2)$$

Equation for ion pressure:

$$\frac{\partial}{\partial t} P_i + \vec{V} \cdot_i \nabla P_i + \tau P_i \cdot \nabla \cdot \vec{V}_i = 0 \qquad (3)$$

Adiabatic electrons: $n_e(x) = n(0) e^{e\phi/T_e}$ (4)

Quasineutrality condition: $n_i = n_e$ (5)

2）Drift approximation：

magnetized plasma： $\delta \equiv \rho / L << 1$

drift approximation： $\frac{\partial}{\partial t} \sim \delta \frac{V_t}{L}$

lowest order：left side of Eq.（2）equals zero & neglecting the viscosity term give,

$$en_i\left(-\nabla\phi+\frac{\vec{V}_i}{c}\times\vec{B}\right)-\nabla P_i=0 \qquad (2a)$$

$\hat{b}\times(2a)$ gives：

$$\vec{V}_i^{(0)}=V_{\parallel}\hat{b}+\frac{c}{b}\hat{b}\times\nabla\phi+\frac{c}{eBn}\hat{b}\times\nabla P_i \qquad (6)$$

where $\hat{b} \equiv \frac{\vec{B}}{B}$

Substituting Eq.(6) into the right side of Eq.（2）， up to the first order of drift approximation we get ,

$$\vec{V}_i^{(1)} = -\frac{m_i c^2}{eB^2}\left(\frac{\partial}{\partial t} + \vec{V}_i^{(0)} \cdot \nabla\right)\nabla_\perp \phi \qquad (7)$$

where gyro-viscosity cancelation (Horton, Phys,Fluids 1971,P116) has been applied.

$\hat{b}$(2) gives

$$\hat{b} \cdot m_i n_i \left(\frac{\partial}{\partial t} + \vec{V}_i \cdot \nabla\right)\vec{V}_i = en_i \hat{b} \cdot \nabla \phi - \hat{b} \cdot \nabla P_i - \hat{b} \cdot \nabla \cdot \vec{\Pi} \qquad (8)$$

3)Linearization

$$n = n_0 + \tilde{n}, \qquad \frac{d}{dt} = \frac{\partial}{\partial t} + \vec{V}_i^{\,0} \cdot \nabla, \qquad V_\parallel = V_{0\parallel} + \tilde{V}_\parallel,$$

$$\vec{V}_\perp = \frac{c}{B}\hat{b} \times \left(\nabla\phi + \frac{1}{en}\nabla\tilde{P} \right) - \frac{c}{\Omega B}\frac{d}{dt}\nabla_\perp\phi + \frac{c}{eBn}\hat{b} \times \nabla P_0.$$

Normalization: $\hat{n} = \tilde{n} / n_0$

After linearization, Eq.(1) becomes,

$$\frac{\partial\hat{n}}{\partial t} + V_{0\parallel}\hat{b}\cdot\nabla\hat{n} + \hat{b}\cdot\nabla\tilde{V}_\parallel + \frac{c}{B}\left[\hat{b}\times\nabla\phi\cdot\nabla\ln n_0\right] - \frac{c}{B\Omega}\frac{d}{dt}\nabla_\perp^2\phi = 0 \qquad (16)$$

Equation （8） becomes:

$$\frac{\partial\hat{V}_\parallel}{\partial t} + V_{0\parallel}\hat{b}\cdot\nabla\hat{V}_\parallel + \frac{c}{B}\hat{b}\times\nabla\phi\cdot\nabla\ln V_{0\parallel} = -\frac{-e}{m_i V_{0\parallel}}\hat{b}\cdot\left(\nabla\phi + \frac{P_0}{en_0}\nabla\hat{P}\right), \qquad (17)$$

Eq.（3）reduces to

$$\frac{\partial \hat{P}}{\partial t}+V_{0\parallel}\hat{b}\cdot\nabla\hat{P}+\frac{c}{B}\hat{b}\times\nabla\varphi\cdot\nabla\ln P_0+\Gamma\nabla\cdot\hat{\tilde{V}}=0 \tag{18}$$

Neglecting the forth term and putting $\tilde{f} = fe^{-i\omega t+i\vec{k}\cdot\vec{r}}$ give,

$$\hat{P}=\frac{\frac{c}{B}\hat{b}\times\nabla\varphi\cdot\nabla\ln P_0}{i(\omega-V_{0\parallel}k_\parallel)} \tag{19}$$

$$\tilde{V}_\parallel=\frac{1}{i\left(\omega-k_\parallel V_{0\parallel}\right)}\left\{\frac{c}{B}\hat{b}\times\nabla\phi\cdot\nabla\ln V_{0\parallel}+\frac{e}{mV_{0\parallel}}\hat{b}\cdot\left[\nabla\phi+\frac{P_0}{en_0}\nabla\left(\frac{\frac{c}{B}\hat{b}\times\nabla\phi\cdot\nabla\ln P_0}{i\left(\omega-k_\parallel V_{0\parallel}\right)}\right)\right]\right\} \tag{20}$$

Substituting Eq.（19）and（20）into Eq.（16），we get

$$\frac{\partial\hat{n}}{\partial t}+V_{0\parallel}\hat{b}\cdot\nabla\hat{n}+\frac{V_{0\parallel}}{i\left(\omega-V_{0\parallel}k_\parallel\right)}\hat{b}\cdot\nabla$$
$$\left\{\frac{c}{B}\hat{b}\times\nabla\varphi\cdot\nabla\ln V_{0\parallel}+\frac{e}{mV_{0\parallel}}\hat{b}\cdot\left[\nabla\varphi+\frac{P_0}{en_0}\nabla\left(\frac{\frac{c}{B}\hat{b}\times\nabla\varphi\cdot\nabla\ln P_0}{i\left(\omega-k_\parallel V_{0\parallel}\right)}\right)\right]\right\}+$$
$$+\frac{c}{B}\left(\hat{b}\times\nabla\varphi\cdot\nabla\ln n_0\right)-\frac{c}{B\Omega}\frac{d}{dt}\nabla_\perp^2\phi=0 \tag{21}$$

From quasi-neutrality condition and adiabatic electron response, we get

$$\left\{\frac{\omega - k_{\|}V_{0\|} - \omega_{*e}}{\omega - k_{\|}V_{0\|} + \omega_{*e}(1+\eta_i)\,{}^{T_i}\!/_{T_e}} + \frac{\omega_{*e} k_{\|} V_{0\|}' L_n}{(\omega - k_{\|}V_{0\|})\left[\omega - k_{\|}V_{0\|} + \omega_{*e}(1+\eta_i)\right]{}^{T_i}\!/_{T_e}} - \frac{c_s^2 k_{\|}^2}{(\omega - k_{\|}V_{0\|})^2} - \rho_s^2 \nabla_{\perp}^2\right\}\phi = 0 \qquad (22)$$

In a sheared slab geometry,

$$\vec{B} = B_0\left(\hat{e}_Z + \frac{x}{L_s}\hat{e}_y\right), \qquad k_{\|} = \frac{k_y x}{L_s}$$

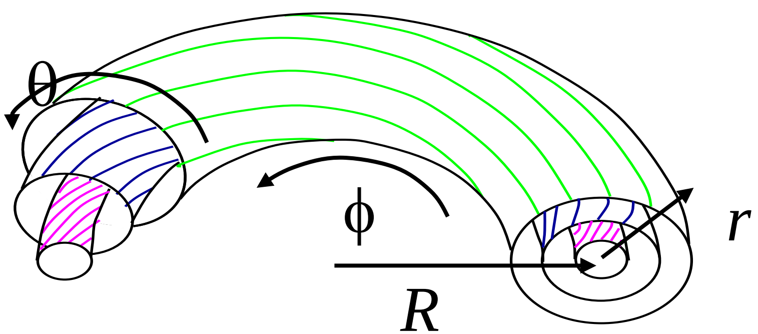

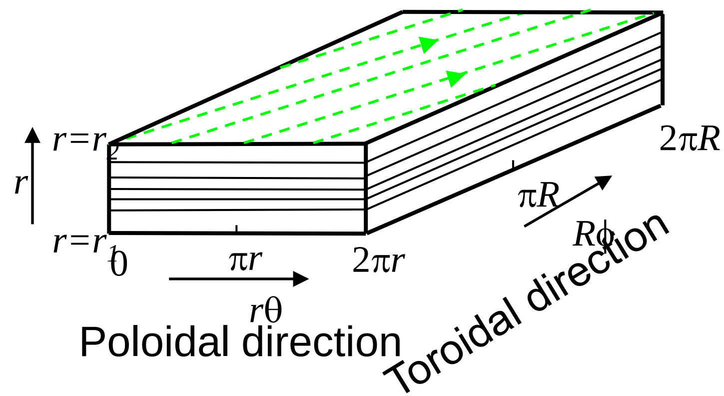

Neglecting $V_{0\|}$ which induce Doppler shift only， then we get dispersion equation：

$$\{\frac{d^2}{dx^2}-k_y^2\rho_s^2+\frac{1-\hat{\omega}}{\hat{\omega}+(1+\eta_i)T_i/T_e}-$$

$$-\frac{xL_nV_{0\|}'/c_s}{\hat{\omega}\left[\hat{\omega}+(1+\eta_i)\right]T_i/T_e}+\frac{(L_n/L_s)^2x^2}{\hat{\omega}^2}\}\varphi(x)=0$$

(23)

where, $\hat{\omega}=\dfrac{\omega}{\omega_{*e}}$ ， x is normalized to ρ_s

If $V_{0\|}'=0$, Eq.（23）reduces to

$$\{\frac{d^2}{dx^2}-k_y^2\rho_s^2+\frac{1-\hat{\omega}}{\hat{\omega}+(1+\eta_i)T_i/T_e}+\left(\frac{L_n}{L_s}\right)^2\frac{x^2}{\hat{\omega}^2}\}\varphi(x)=0.$$

This is a standard Weber equation, its eigen-value equation is,

$$\left[-k_y^2\rho_s^2+\frac{1-\hat{\omega}}{\hat{\omega}+\left(1+\eta_i\right)T_i/T_e}\right]\frac{\hat{\omega}}{is}=2n+1.$$

The corresponding eigen-function is,

$$\phi^{(n)}(x)=\phi_0^{(n)}H_n\left(\sqrt{is/\hat{\omega}}\cdot x\right)e^{-isx^2/2\hat{\omega}}$$

where H is the Hermite Polynomial, $\hat{s}=L_n/L_s$

We usually consider $n=0$ only and $H_0=1$

n>1 harmonics may be important when gradients are high.

.

Weber equation

$$\left[\frac{d^2}{dx^2}+a+bx^2\right]y(x)=0$$

Eigen-value equation, $a=i(2n+1)\sqrt{b}$

Corresponding eigen-function, $y(x)=H_n\left(i\sqrt{b}x\right)e^{-ibx^2/2}$

$$\begin{cases} y''+\left(2n+1-x^2\right)y=0 \\ y=e^{-x^2/2}H_n(x) \end{cases}$$

Home work: if $V'_{0\|}\neq 0$ ， what are the eigen-value equation and eigen-function？ [Reference, Dong et al, Phys. Plasmas 1, 3250(1994).]

(5)Kinetic study of temperature gradient modes

1) Particle orbit in a sheared slab geometry

$$\vec{B} = B_0\left(\hat{Z} + \frac{x}{L_s}\hat{y}\right)$$

Motion of charged particles：

$$\frac{d\vec{r}\,'}{dt'} = \vec{V}'$$

$$\frac{d\vec{V}'}{dt'} = \frac{q}{mc}\vec{V}' \times \vec{B}$$

Assuming $\vec{r}\,' = \vec{r},\ \vec{V}' = \vec{V},$ **when** $t' = t$ **, the solution of above equations are**

$$V_x'(t') = V_\perp \cos[\theta - \Omega(t'-t)]$$

$$V_y'(t') = V_\perp \sin[\theta - \Omega(t'-t)]$$

$$V_z'(t') = V_z$$

$$x'(t') - x = -\frac{V_\perp}{\Omega}[\sin[\theta - \Omega(t'-t)] - \sin\theta]$$

$$y'(t') - y = \frac{V_\perp}{\Omega}[\cos[\theta - \Omega(t'-t)] - \cos\theta]$$

$$z'(t') - z = V_z(t'-t)$$

Constants of particle motion:

$$\alpha = V_x^2 + V_y^2$$

$$\beta = (V_z - V)^2$$

$$\gamma = x + \frac{V_y}{\Omega} \equiv X_g, \text{ where } \Omega = \frac{eB}{mc} \cong \frac{eB_0}{mc},$$

2) distribution function:

Vlasov equation : $\frac{\partial f}{\partial t} + \vec{V}\cdot\nabla f + \frac{q}{m}\left(\vec{E} + \frac{1}{c}\vec{V}\times\vec{B}\right)\cdot\nabla_V f = 0$

Linearization $f = f_0 + f_1$

f_0 ~ **zeroth order distribution function, satisfying**

Zeroth order equation $\frac{df_0}{dt} = 0,$

$$f_0 = f_0(\text{const. of motion})$$

$$f_0 = n_0\left(\frac{m}{2\pi T}\right)^{3/2} e^{-m\left(V_\parallel^2 + V_\perp^2\right)/2T}, \quad \begin{aligned} n_0 &= n_0\left(X_g\right) \\ T &= T\left(X_g\right) \end{aligned}$$

The first order equation (electrostatic perturbation)

$$\frac{\partial f_1}{\partial t} + \vec{V} \cdot \nabla f_1 + \frac{e}{m}\left(\vec{V} \times \vec{B}_0\right) \cdot \nabla_V f_1 + \frac{e}{m} \vec{E}_1 \cdot \nabla_V f_0 = 0$$

$$\frac{df_1}{dt} = \frac{e}{m} \nabla \phi \cdot \nabla_V f_0, \qquad \vec{E}_1 = -\nabla \tilde{\varphi}$$

$$\nabla_V f_0 = \frac{\partial f_0}{\partial \alpha} \nabla_V \alpha + \frac{\partial f_0}{\partial \beta} \nabla_V \beta + \frac{\partial f_0}{\partial \gamma} \nabla_V \gamma$$

$$= -\frac{m}{T} \vec{v} f_0 + \hat{y} \frac{1}{\Omega} \frac{\partial f_0}{\partial \gamma}$$

$$\frac{d\varphi}{dt} = \frac{\partial \varphi}{\partial t} + \vec{V} \cdot \nabla \varphi$$

The equation for the first order distribution function

$$\frac{df_1}{dt} = -\frac{e}{T}\left[\left(\frac{d\varphi}{dt} - \frac{\partial \varphi}{\partial t}\right) f_0 - \frac{T}{m\Omega} \hat{y} \cdot \nabla \varphi \frac{\partial f_0}{\partial \gamma}\right]$$

3）Perturbation of distribution function

$$f_1 = f_1(x,\vec{V})e^{-i\omega t+ik_y y+ik_z z}$$

$$\varphi = \varphi(x)e^{-i\omega t+ik_y y+ik_z z}$$

$$f_1(x,\vec{V}) = -\frac{e}{T}\{\phi(x)\, f_0 + \left[i\omega f_0 - \frac{ik_y}{m\Omega}\frac{\partial f_0}{\partial \gamma}\right]\int_{-\infty}^{t}\phi(x')dt' \times$$

$$\exp\left[-i\omega(t'-t)+ik_y(y'-y)+ik_z(z'-z)\right]\}$$

$$\frac{\partial f_0}{\partial \gamma} = \frac{\partial f_0}{\partial X_g} = \left(\frac{dn}{dX_g}\frac{1}{n} + \frac{dT}{dX_g}\frac{\partial}{\partial T}\right) f_0,$$

For ions

$$\frac{\partial f_0}{\partial \gamma} = -\omega_{*e}\left[\frac{1}{\tau_i} + \frac{\eta_i}{\tau_i}\left(\hat{V}_{\parallel}^2 + \hat{V}_{\perp}^2 - \frac{3}{2}\right)\right]$$

where

$$\omega_{*e} = \frac{ck_y T_e}{eBL_n},\ \tau_i = \frac{T_e}{T_i}, \eta_i = \frac{L_n}{L_{T_i}},\quad L_n = -\left(\frac{1}{n_0}\frac{dn_0}{dX_g}\right)^{-1},\quad L_{T_i} = \left(\frac{1}{T_i}\frac{dT_i}{dX_g}\right)^{-1},\quad \hat{V} = \frac{V}{V_{th}}.$$

4) Dispersion equation

$$n_i = n_{i0} + n_{i1}, \quad n_{i1} = \int f_1 d\vec{V},$$

$$n_{i1} = n_{i1}(x) e^{-i\omega t + ik_y y + ik_z z}$$

$$= -\frac{e}{T_i}\{n\phi(x) + \int d\vec{V}\left[i\omega + \frac{ik_y}{m\Omega}\omega_{ne}^*\left(\frac{1}{\tau_i} + \frac{\eta_i}{\tau_i}\left(\hat{V}_\parallel^2 + \hat{V}_\perp^2 - \frac{3}{2}\right)\right)\right] f_0 \times$$

$$\int_{-\infty}^{t} \phi(x')dt' \exp\left[-i\omega(t'-t) + ik_y(y'-y) + ik_z(z'-z)\right]\}$$

Applying expansions

$$\exp(ia\cos\theta) = \sum_{n=-\infty}^{\infty} (i)^n J_n(a)\exp(iw\theta), \quad and$$

$$\exp(-ia\cos\theta) = \sum_{n=-\infty}^{\infty} (-i)^n J_n(a)\exp(-in\theta),$$

and Fourier transform

$$\hat{n}_{i1}(k) = \int \frac{dx}{\sqrt{2\pi}} n(x) e^{-ikx} dx$$

We get

$$\hat{n}_{i1}(k) = -\frac{en_0}{T_i}\hat{\phi}(k) - \frac{ie}{T}\int \frac{dk'}{\sqrt{2\pi}}\hat{\phi}(k')\int \frac{dx}{\sqrt{2\pi}} e^{i(k'-k)x}\int_{-\infty}^{0} H(\tau)d\tau$$

where,

$$H = \frac{n_0}{\pi^{3/2}} \int d\hat{\vec{V}} e^{-\left(\hat{V}_\parallel^2 + \hat{V}_\perp^2\right) + i\left(k_\parallel V_\parallel - \omega\right)\tau} J_0\left(k_\perp V_\perp / \Omega\right) J_0\left(\frac{k'_\perp V_\perp}{\Omega}\right) F$$

$$F = \omega_{*e}\left[\hat{\omega} + \frac{1}{\tau_i} + \frac{\eta_i}{\tau_i}\left(\hat{V}_\parallel^2 + \hat{V}_\perp^2 - \frac{3}{2}\right)\right]$$

Applying the formula

$$\int_0^\infty e^{-\sigma^2 x^2} J_m(\alpha x) J_m(\beta x)\, x dx = \frac{1}{2\sigma^2} \exp\left(-\frac{\alpha^2 + \beta^2}{4\sigma^2}\right) I_m\left(\frac{\alpha\beta}{2\sigma^2}\right),$$

$$\int_0^\infty e^{-\sigma^2 x^2} J_m(\alpha x) J_m(\beta x) \frac{x^2}{2} x dx = f_m(b, b_1) I_m(b) e^{-b_1}.$$

where

$$f_m(b, b_1) = (1 - b_1) + b I'_m(b) / I_m(b),$$

$$b = \frac{\alpha\beta}{2\sigma^2}, \quad b_1 = \frac{\alpha^2 + \beta^2}{4\alpha^2}.$$

$$\hat{n}_{i1}(k) = -\int \frac{dk'}{\sqrt{2\pi}} \hat{\phi}(k') \int \frac{dx}{\sqrt{2\pi}} e^{i(k'-k)x} P_i(k'_1, k) \cdot \frac{en_0}{T_i} - \frac{en_0}{T_i} \hat{\phi}(k)$$

where

$$P_i\left(k',k\right)=\{\zeta_i Z\left(\zeta_i\right)\tau_i+\frac{\omega_{*e}}{k_{\|}V_{ti}}[Z\left(\zeta_i\right)+\eta_i\left(\left(-b_{1i}+\frac{bI_{1i}}{I_{0i}}-\frac{1}{2}\right)Z\left(\zeta_i\right)\right)+\zeta_i\left(1+Z\left(\zeta_i\right)\right)]\}\Gamma_{0i}\left(k_\perp,\right.$$

$$\varsigma_i=\frac{\omega}{k_{\|}V_{ti}},\quad b_i=\frac{k_\perp k'_\perp\rho_i^2}{2},\quad b_{1i}=\frac{\left(k_\perp^2+k_\perp'^2\right)\rho_i^2}{4},\quad k_\perp^2=k_y^2+k^2,\quad k_\perp'^2=k_y^2+k'^2,$$

$$\Gamma_0\left(k_\perp,k'_\perp\right)=I_0\left(b\right)e^{-b_1},\qquad Z\left(\varsigma\right)=\frac{1}{\pi^{1/2}}\int_{-\infty}^{\infty}\frac{\exp\left(-\beta^2\right)}{\beta-\varsigma}d\beta.$$

In the same way we get the electron density perturbation as

$$\hat{n}_{e1}=\frac{en_0}{T_e}\hat{\phi}(k)+\frac{en}{T_e}\int\frac{dk'}{\sqrt{2\pi}}\hat{\phi}(k')\int\frac{dx}{\sqrt{2\pi}}e^{i(k'-k)x}P_e(k',k)$$

From Poison equation,

$$\nabla^2\varphi=-4\pi e\left(\tilde{n}_i-\tilde{n}_e\right)$$

we get integral eigen-value equation,

$$\frac{\Omega_e^2}{2\omega_{pe}^2}k_\perp^2\rho_e^2\phi(k)+\frac{T_e}{n_{0e}q_e^2}\sum_j\frac{q_j^2n_{0j}}{T_j}\left\{\phi(k)+\frac{1}{2\pi}\int dk'\int dx\exp\left[i(k'-k)x\right]H_j\ (k,k')\phi(k')\right\}=0,$$

where,

$$H_j = (1 - \frac{\omega_{*j}}{\omega})\zeta_j Z(\zeta_j)\Gamma_{0j} -$$

$$\eta_j \frac{\omega_{*j}}{\omega}\left\{\left[\zeta_j^2 + (\zeta_j^2 - \frac{1}{2})\zeta_j Z(\zeta_j)\right]\Gamma_{0j} + (\frac{k_\perp k_\perp^{'} \rho_j^2}{2}\Gamma_{1j} - \frac{k_\perp^2 \rho_j^2 + k_\perp^{'2} \rho_j^2}{4}\Gamma_{0j})\zeta_j Z(\zeta_j)\right\},$$

$$\zeta_j = \frac{\omega}{|k_{//}| V_{tj}}.$$

Debey shielding

quasi-neutrality condition:

$$\tilde{n}_i = \tilde{n}_e, \quad \text{or} \quad \tilde{n}_i - \tilde{n}_e = 0,$$

Poinson equation

$$\nabla^2 \phi = -4\pi e(\tilde{n}_i - \tilde{n}_e), \quad \tilde{n} \sim \frac{ne\phi}{T_e},$$

$$k_\perp^2 : \frac{4\pi e^2 n}{T_e} \square\ k_\perp^2 : \frac{1}{\lambda_D^2} \square\ \frac{1}{\lambda_\perp^2} : \frac{1}{\lambda_D^2},$$

if $\lambda^2 >> \lambda_D^2, \nabla^2 \sim k^2$ is negligible.

define $d_s = \frac{\Omega_e^2}{\omega_{pe}^2}$, then $k_\perp^2 \rho_e^2 d_s : 1.$

5）Typical umerical results：

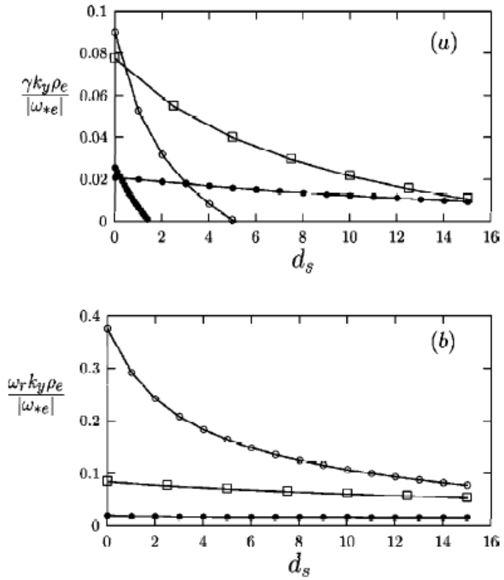

FIG. 1. The normalized mode growth rate (a) and real frequency (b) as functions of Debye shielding parameter $d_s = \Omega_e^2/\omega_{pe}^2$ for $\eta_e = \eta_i = 4$ and $\hat{s} = 0.1$. The lines with closed circles, squares and open circles are for $k_y\rho_e = 0.2$, 0.5, and 1, respectively. The heavy line is for $\eta_e = 4$, $\eta_i = 0$, and $k_y\rho_e = 0.5$.

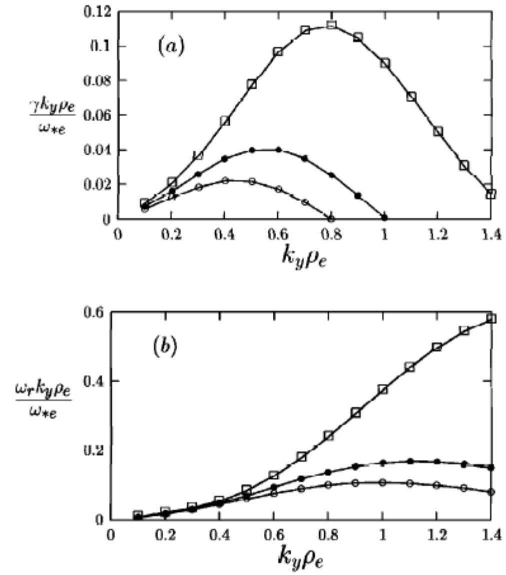

FIG. 2. The normalized mode growth rate (a) and real frequency (b) as functions of $k_y\rho_e$. The lines with squares, closed circles and open circles are for $d_s = 0$, 5, and 10, respectively. The other parameters are the same as in Fig. 1.

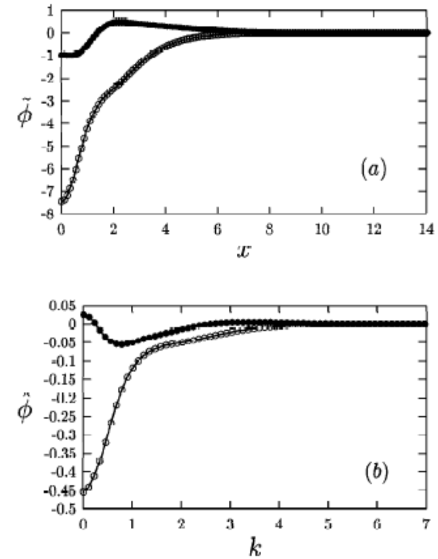

FIG. 3. The eigenfunctions $\tilde{\phi}(x)$ (a) and $\hat{\phi}(k)$ (b) for $d_s = 0$ and $k_y\rho_e = 0.5$. The other parameters are the same as in Fig. 1. The lines with open and closed circles are the real and imaginary parts, respectively.

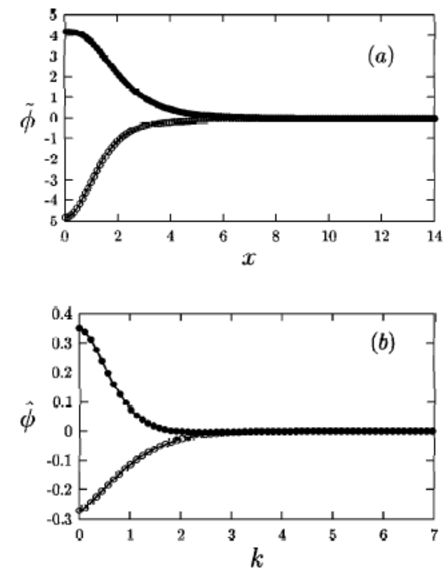

FIG. 4. The same as in Fig. 3 but for $d_s = 10$.

6）Approximate equation without magnetic shear

$$\int_{-\infty}^{\infty} dx e^{i(k'-k)x} = 2\pi\delta(k'-k)$$

The dispersion equation reduces

$$1+\tau_i + \frac{k_{e\perp}\Omega^2{}_e}{2\omega^2{}_{pe}} + P_i(k,k) + P_e(k,k) = 0,$$

$$P_i(k',k) = \{\zeta_i Z(\zeta_i)\tau_i + \frac{\omega_{*e}}{k_\parallel V_{ti}}[Z(\zeta_i) + \eta_i\left(\left(-b_{1i} + \frac{bI_{1i}}{I_{0i}} - \frac{1}{2}\right)Z(\zeta_i)\right)$$

$$+\zeta_i(1+Z(\zeta_i))]\}\Gamma_{0i}(k_\perp, k'_\perp)$$

Home work: under the conditions $\zeta_j = \frac{\omega}{|k_{//}|V_{tj}} >> 1$ and $b_i = \frac{k_\perp k'_\perp \rho_i^2}{2} << 1$, it reduces to fluid equation.

(6) Mode characteristics in a tokamak

1) Toridisity induced drifts：

$$\omega_{*sT} = \omega_{*s}[1+\eta_s(\frac{v^2}{v_{ts}^2}-\frac{3}{2})]$$

$$\omega_{Ds} = 2\frac{L_n}{R}\omega_{*s}[\cos\theta+\sin\theta(\hat{s}\theta-\alpha\sin\theta)](\frac{\hat{v}_\perp^2}{2}+\hat{v}_{//}^2)$$

2）**Linear coupling：** **format of perturbations:**

,

$$\tilde{f} = \sum_{m,n}\tilde{f}_{m,n}(r)e^{-i\omega t+im\theta-in\varsigma}$$

Equilibrium magnetic field：

$$B_\varphi = \frac{B_0}{(1+r\cos\theta/R_0)} \cong B_0(1-r\cos\theta/R_0)$$

Equation for perturbation of distribution function

$$\frac{\partial f_1}{\partial t}+\vec{V}\cdot\nabla f_1+\frac{e}{m}\left(\vec{V}\times\vec{B}_0\right)\cdot\nabla_V f_1+\frac{e}{m}\vec{E}_1\cdot\nabla_V f_0=0$$

m component couples with m+1**and** m-1 **components through equilibrium magnetic field**

3) Ballooning representation (n>>1)

$$\tilde{f}_n = \sum_{m=-\infty}^{\infty} e^{im\theta} \int_{-\infty}^{\infty} e^{-im\theta'} e^{-in(\varsigma - q\theta') - i\omega t} \tilde{f}_n(\theta') d\theta'$$

4)Integral dispersion equation for ETG modes

$$[1 + \tau_{\mathrm{i}} + \frac{k_\perp^2}{2} \frac{\Omega_e^2}{\omega_{pe}^2}]\hat{\varphi}(k) = \int_{-\infty}^{\infty} \frac{dk'}{\sqrt{2\pi}} K(k,k')\hat{\varphi}(k')$$

where

$$K(k,k') = -i\int_{-\infty}^{0} \omega_{*e} d\tau H(k,k'), \quad k = k_\theta \hat{s}\theta, \quad k' = k_\theta \hat{s}\theta'$$

$$\mathrm{H}(k,k') = \sqrt{2} e^{-i\omega\tau} \frac{\exp\left[-\frac{(k'-k)^2}{4\lambda_e}\right]}{\sqrt{a_e}(1+a_e)\sqrt{\lambda_e}} \times \left\{ D_0 - \frac{\eta_e (k-k')^2}{4 a_e \lambda_e} \right\} \Gamma_0(k_\perp, k'_\perp)$$

$$D_0 = \frac{\omega}{\omega_{*e}} - 1 + \frac{3}{2}\eta_e - \frac{2\eta_e}{1+a_e} \times \left[1 - \frac{k_\perp^2 + k_\perp'^2}{2(1+a_e)} + \frac{k_\perp k'_\perp I_1}{(1+a_e) I_0} \right]$$

$$\lambda_e = \frac{\tau^2 \omega_{*e}^2}{a_e} \left(\frac{\hat{s}}{q} \varepsilon_n \right)^2, \quad a_e = 1 - i2\varepsilon_n \omega_{*e} \tau \frac{g(\theta,\theta')}{\theta - \theta'}, \quad \alpha = -R_0 q^2 \frac{d\beta}{dr}$$

$$g(\theta,\theta') = (\hat{s}+1)(\sin\theta - \sin\theta') - \hat{s}(\theta\cos\theta - \theta'\cos\theta') - \frac{\alpha}{2}(\theta - \theta' - \sin\theta\cos\theta + \sin\theta'\cos\theta')$$

5)Electromagnetic instabilities

$$[1+\tau_i]\hat{\phi}(k) = \int_{-\infty}^{+\infty} \frac{dk'}{\sqrt{2\pi}} \{K_{11}^i(k,k')\hat{\phi}(k') + [K_{12}^i(k,k') + K_{12}^e(k,k')]\hat{A}_{\parallel}(k')\}, \quad (12)$$

$$\frac{1}{2\tau_i} k_{\perp}^2 \hat{A}_{\parallel}(k) = \int_{-\infty}^{+\infty} \frac{dk'}{\sqrt{2\pi}} \{[K_{21}^i(k,k') + K_{21}^e(k,k')]\hat{\phi}(k') + [K_{22}^i(k,k') + K_{22}^e(k,k')]\hat{A}_{\parallel}(k')\}, \quad (13)$$

$$K_{mn}^i(k,k') = -i\int_{-\infty}^{0} \omega_{*e}\, d\tau\, H_{mn}^i(\tau,k,k'), \quad (14)$$

for $m=1,2$ and $n=1,2$. Here,

$$H_{12}^i(\tau,k,k') = \frac{1}{2\sqrt{a\lambda}}(k-k')H_{11}^i(\tau,k,k'),$$

$$H_{21}^i(\tau,k,k') = -\frac{\beta_i}{2\sqrt{a\lambda}}(k-k')H_{11}^i(\tau,k,k'),$$

$$H_{22}^i(\tau,k,k') = -\frac{\beta_i}{4a\lambda}(k-k')^2 H_{11}^i(\tau,k,k'),$$

$$K_{12}^e(k,k') = \frac{iq\sqrt{\pi\tau_i}}{2\sqrt{2}\epsilon_n\hat{s}}(\hat{\omega}-1)\,\mathrm{sgn}(k-k'),$$

$$K_{21}^e(k,k') = -\frac{\beta_i}{\tau_i}K_{12}^e(k,k'),$$

$$K_{22}^e(k,k') = \beta_i\left\{-\frac{\sqrt{\pi}}{4\sqrt{2}}\left(\frac{q}{\epsilon_n\hat{s}}\right)^2 \hat{\omega}(\hat{\omega}-1)|k-k'| + \frac{\sqrt{\pi}q^2k_\theta}{2\sqrt{2}\hat{s}\epsilon_n}(\hat{\omega}-(1+\eta_e)) \times \mathrm{sgn}(k-k')g(\theta,\theta')\right\};$$

- **Code**: **HD7**
- **Input parameters:**

$$\eta_{i,e}=\frac{L_n}{L_{Te}},\ \varepsilon_n=\frac{L_n}{R},\ \tau_i=\frac{T_e}{T_i},\ q,\ \hat{s}=\frac{rdq}{qdr},\ k_\theta\rho,\ \beta_{e,i},\ \varepsilon=\frac{r}{R}.$$

- **Output: real frequency, growth rate and eigen-function.**
- **Reference: J.Q. Dong, W. Horton, and J.Y. Kim, Phys. Fluids B4, 1867 (1992).**

Topics studied

（i） impurity effects:

i） J. Q. Dong, W. Horton, X. N. Su, Impurity effect on kinetic mode in tokamak plasmas, US-Japan Workshop on ion temperature driven turbulent transport, Austin Texas, January 1993 [AIP Conf. Proc. **284**, 486 (1994)].

ii) J.Q. Dong, W. Horton, Study of Impurity Mode and Ion Temperature Gradient Mode in Toroidal Plasmas, Phys. Plasmas **2**, 3412 (1995).

iii) J.Q. Dong, W. Horton, and W. Dorland, Isotope Scaling and Mode with Impurities in Tokamak Plasmas, Phys. Plasmas **1**, 3635 (1994).

iv) X. Y. Fu, J. Q. Dong, W. Horton, Y.C. Tong, and G.J. Liu, Impurity Transport from the ITG Mode in Toroidal Plasmas, Phys. Plasmas **4**, 588(1997).

v) Huarong Du, Zheng-Xiong Wang, J. Q. Dong, and S. F. Liu, Coupling of ion temperature gradient and trapped electron modes in the presence of impurities in tokamak plasmas, Physics of Plasmas **21**, 052101 (2014).

（ii）trapped electrons(bounce average)

i) J. Q. Dong, S. M. Mahajan, and W. Horton, Coupling of ITG and Trapped Electron Modes in Plasmas with Negative Magnetic Shear, Phys. Plasmas **4**, 755 (1997).

(iii) Velocity shear：

i) J.Q. Dong, W. Horton, Kinetic Quasi-toroidal Ion Temperature Gradient Instability in the Presence of Sheared Flows, Phys. Fluids **B5**,1581 (1993).

(iv) Anisotropy of ion temperature：) J. Q. Dong, Y. X. Long and K. Avinash, Magnetic and Velocity Shear Effects on Modes in Plasmas with Ion Temperature Anisotropy , Phys. Plasmas **8**, 4120 (2001).

(v) Magnetic perturbation(**AITG, KSA,KB)**

i) J.Q. Dong, L. Chen, F. Zonca, Study of Kinetic Shear Alfven Modes Driven by Ion Temperature Gradient in Tokamak Plasmas, Nucl. Fusion, **39**, 1041 (1999).

ii) J. Q. Dong, L. Chen, F. Zonca, and G. D. Jian, Study of kinetic shear Alfven instability in tokamak plasmas, Phys. Plasmas **11**, 997 (2004).

(vi) Elongated cross section

i) Huarong Du, Zheng xiong Wang, and J.Q. Dong, Impurity effects on short wavelength ion temperature gradient mode in elongated tokamak plasmas Physics of Plasmas,20, 022506 (2015).

(vii) Reversed filed pinch configuration

i) Songfen Liu, S.C.Guo, J.Q.Dong, Toroidal kinetic -mode study in reversed-field pinch plasmas, Physics of Plasmas 17， 052505 (2010).

ii) S. Cappello, D. Bonfiglio, D.F. Escandeet al.， Equilibrium and transport for quasi-helical reversed field pinches, Nucl. Fusion **51,** 103012 (2011).

iii) S. F. Liu, C. L .Zhang, W. Kong, S.C. Guo, J.Q. Dong, L.M. Liu, Q.Liu and Z.Y. Liu, Gyrokinetic study of impurity mode in reversed-field pinch, European Phys. Lett. **97**, 55004 (2012).

iv) S.F. Liu, S.C. Guo, W. Kong and J.Q. Dong, Trapped electron effects on η_i-mode and trapped electron mode in RFP plasmas, Nucl. Fusion **54**, 043006 (2014).
v) S.F. Liu, S.C. Guo, C.L. Zhang, J.Q. Dong, L. Carraro and Z.R.Wang, Impurity effects on the ion temperature gradient mode in reversed-field pinch plasmas, Nucl. Fusion **51,** 083021 (2011).

Coupling of ITG and TEM

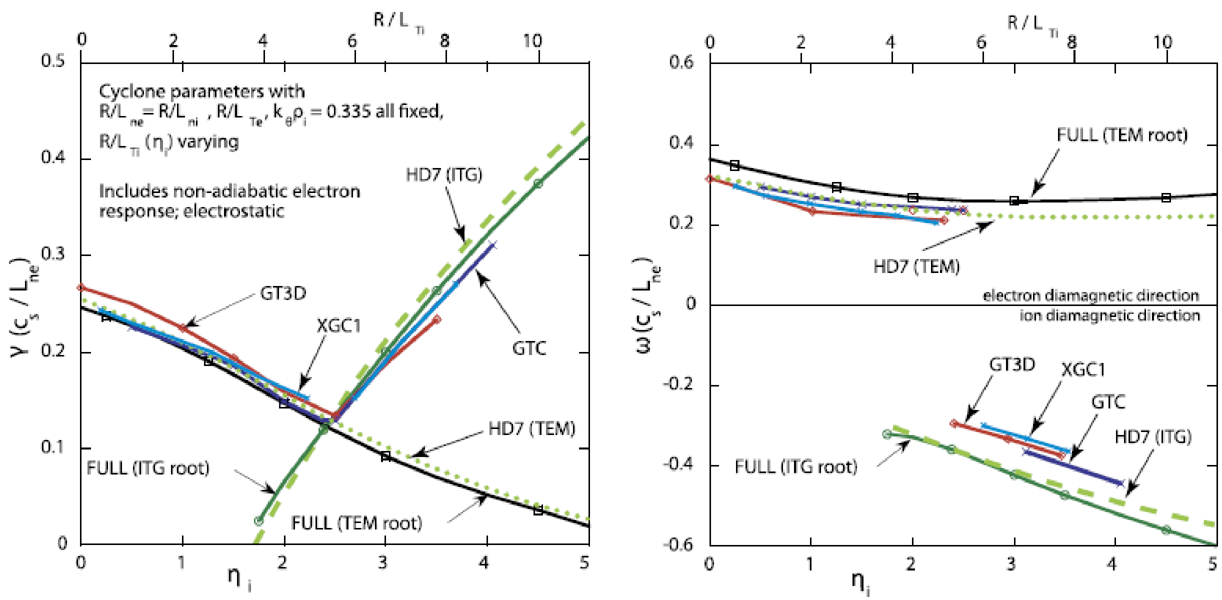

FIG. 1. Linear growth rate γ and real frequency ω of electrostatic ITG and CTEM modes as a function of η_i. GTC, GT3D, and FULL data from Ref. 29, HD7 data from Ref. 31, and XGC1 data from Chang and Ku (Ref. 33).

Holod and Z. Lin, Physics of Plasmas **20,** 032309 (2013)

Electromagnetic modes in pedestal

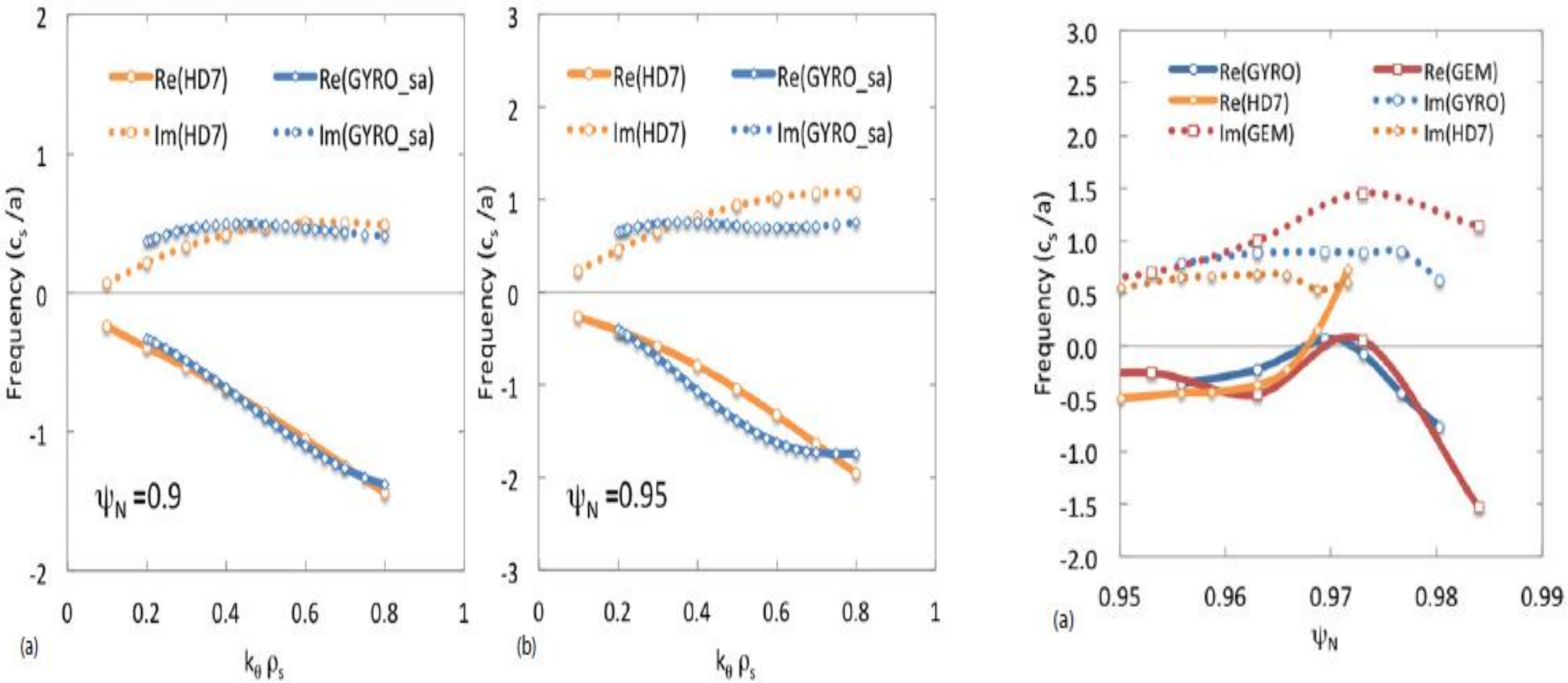

Figure 13. (a) GYRO and HD7 growth rate and real frequency (in units of c_s/a) using GYRO's generated equilibrium parameters for $s-\alpha$ shaping at (a) $\psi_N = 0.9$ and (b) $\psi_N = 0.95$.

E. Wang, X. Xu, J. Candy, R. J. Groebner, P. B. Snyder, Y. Chen, S. E. Parker, W. Wan, Gaimin Lu and J. Q. Dong, Linear gyrokinetic analysis of a DIII-D H-mode pedestal near the ideal ballooning threshold. Nuclear Fusion **52**, 103015 (2012).

Threshold calculation（1）

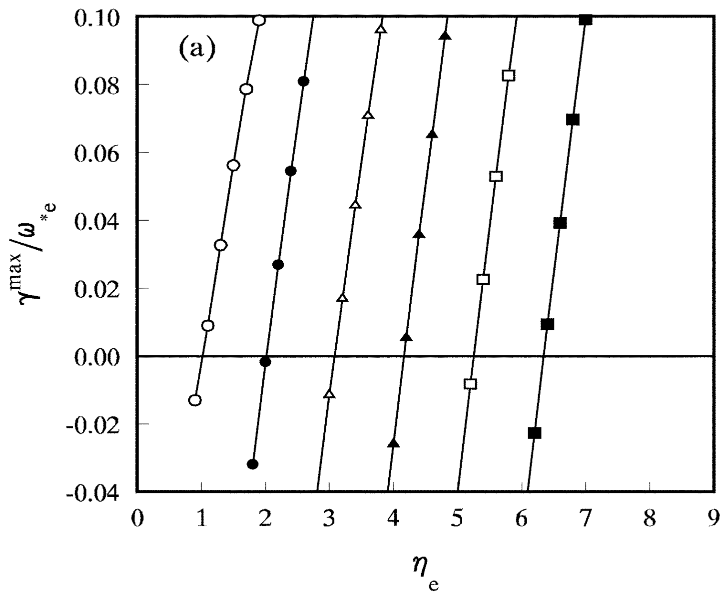

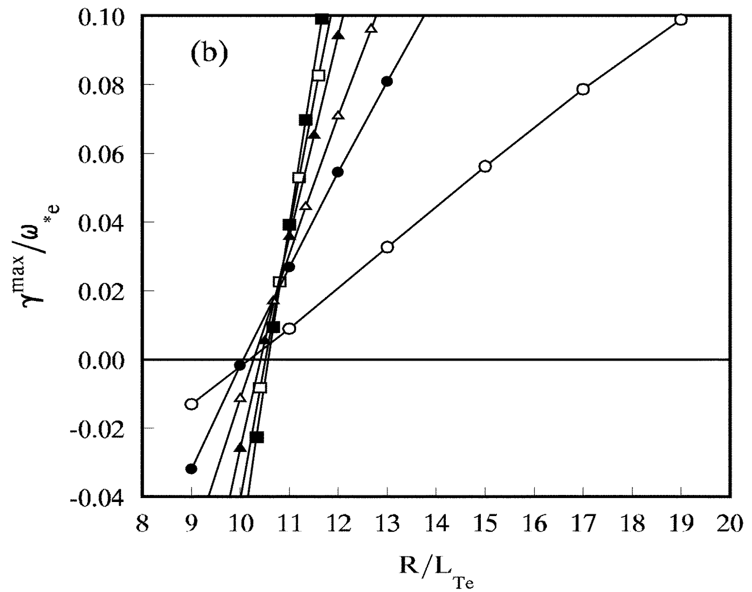

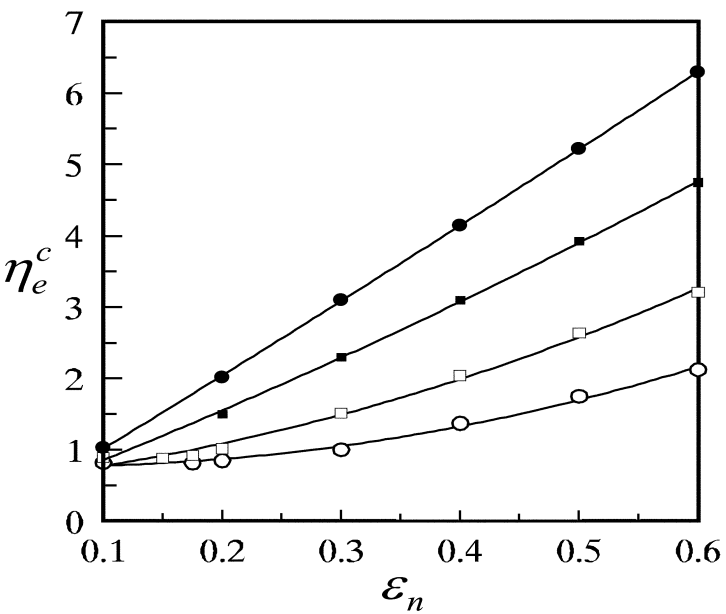

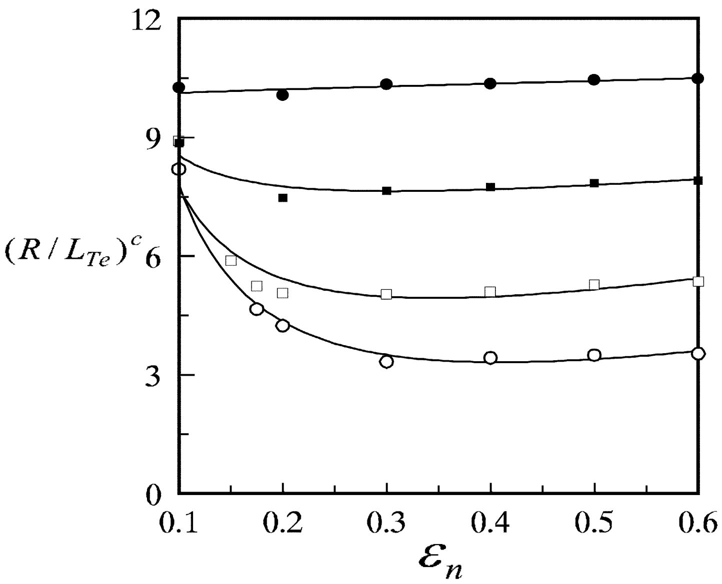

Threshold calculation（2）

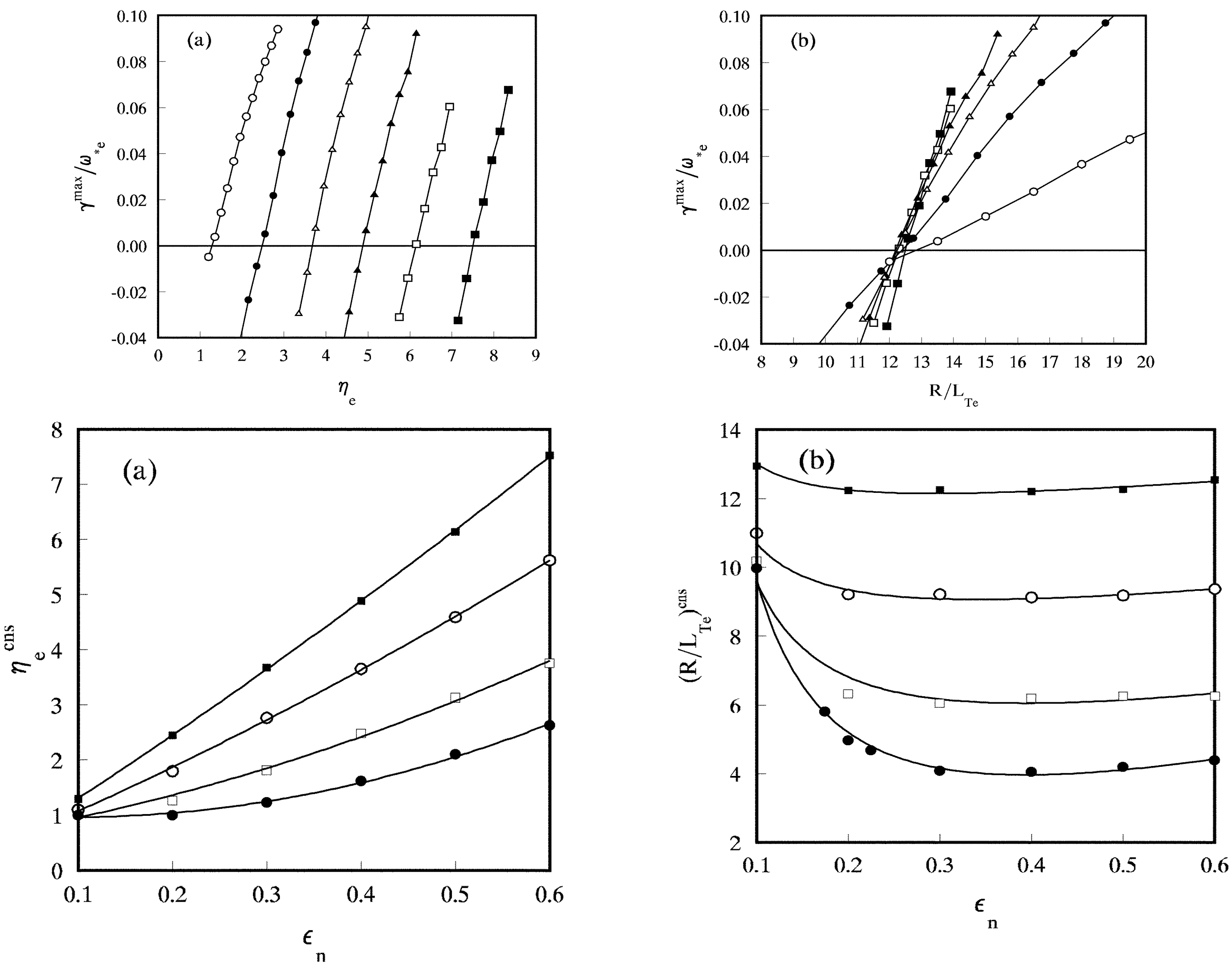

χ_e threshold from experiment

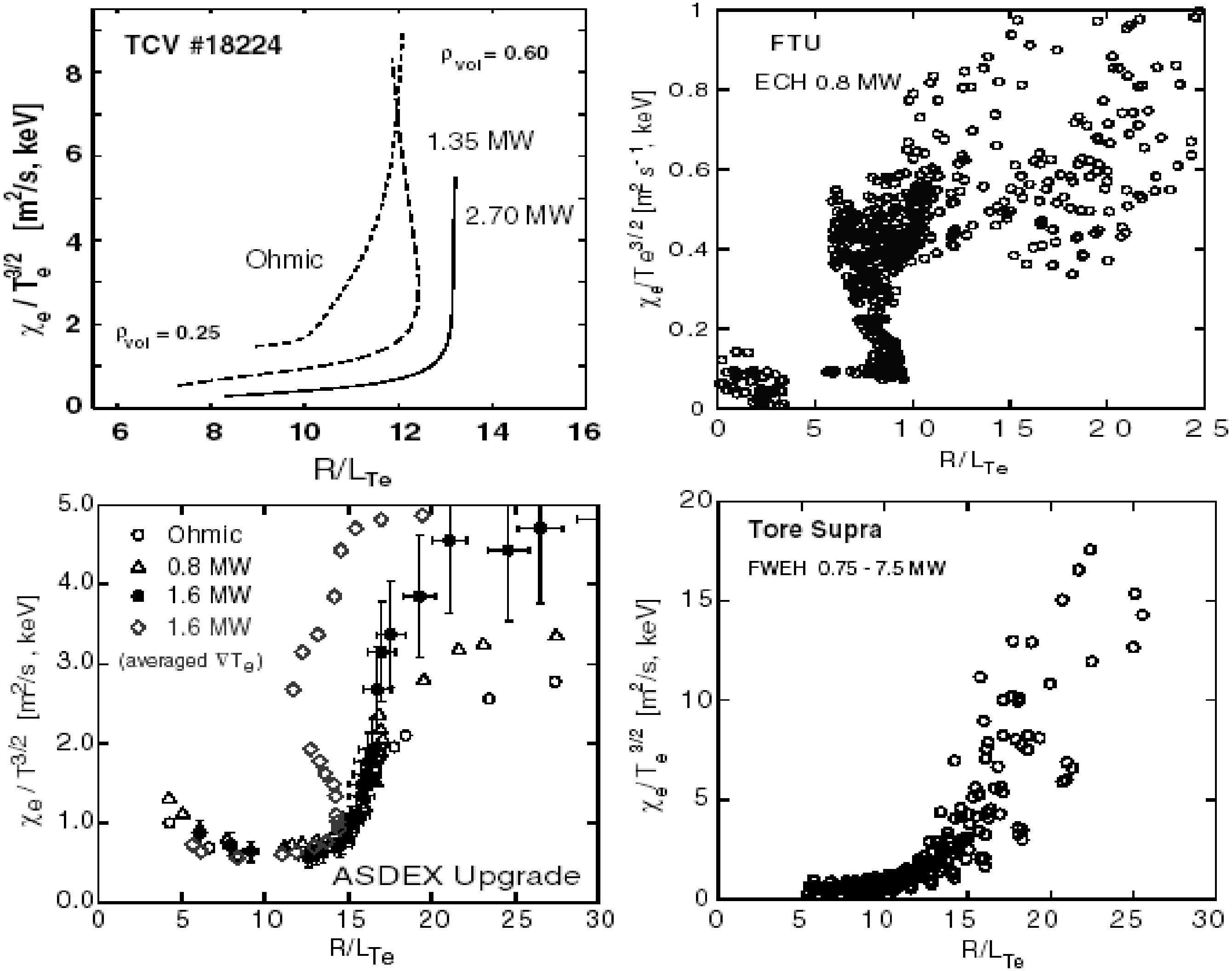

Te critical vs. Te/Ti & R/Ln

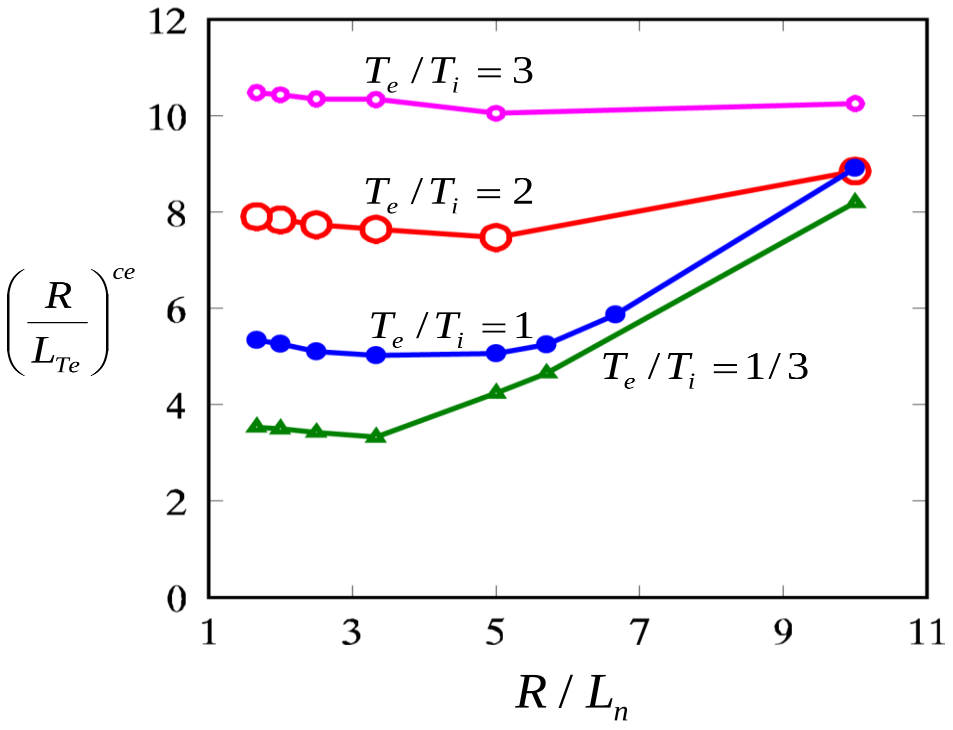

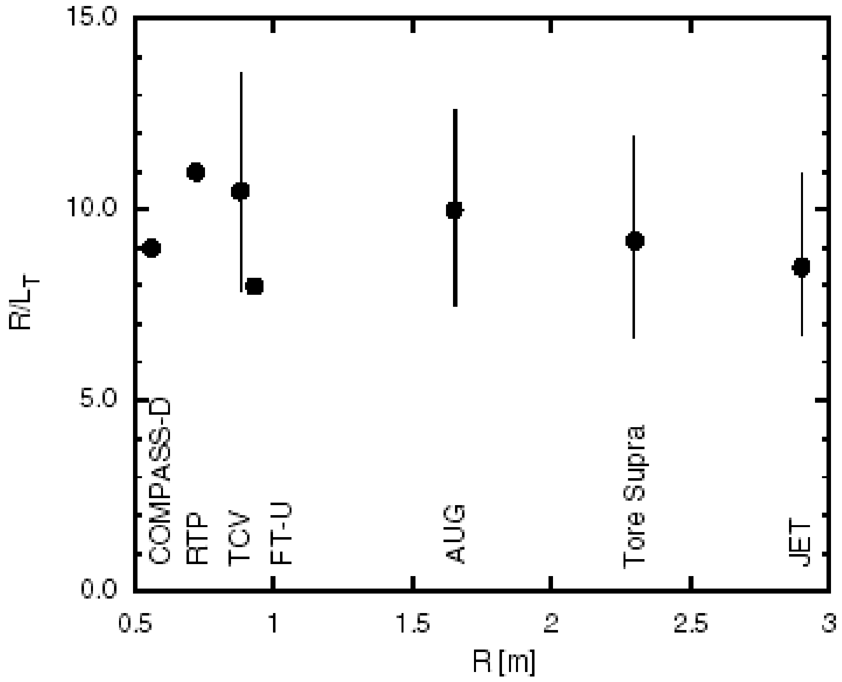

Isotope effect

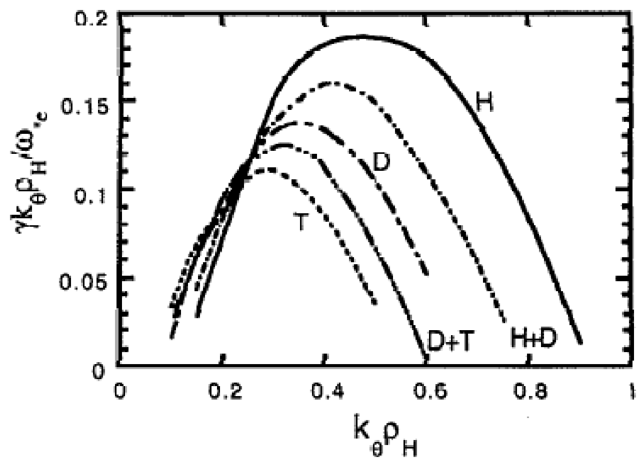

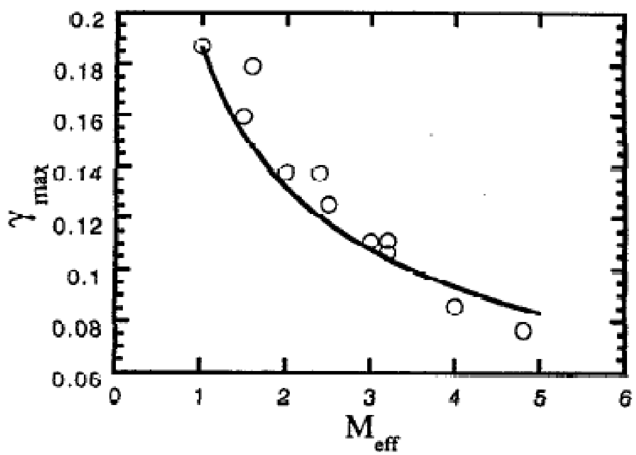

J.Q. Dong, W. Horton, and W. Dorland, Phys. Plasmas 1, 3635 (1994).

finite β effect

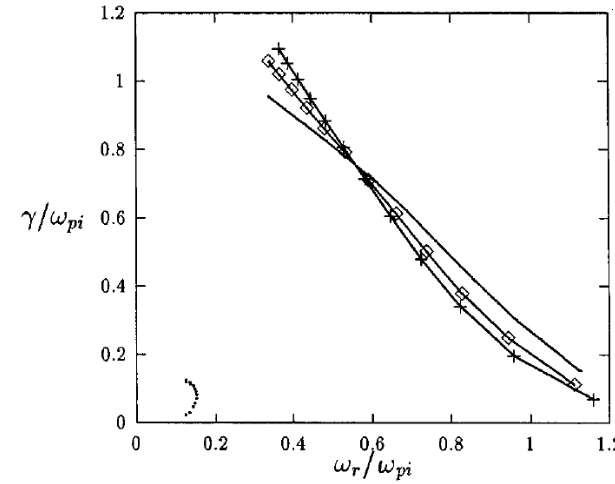

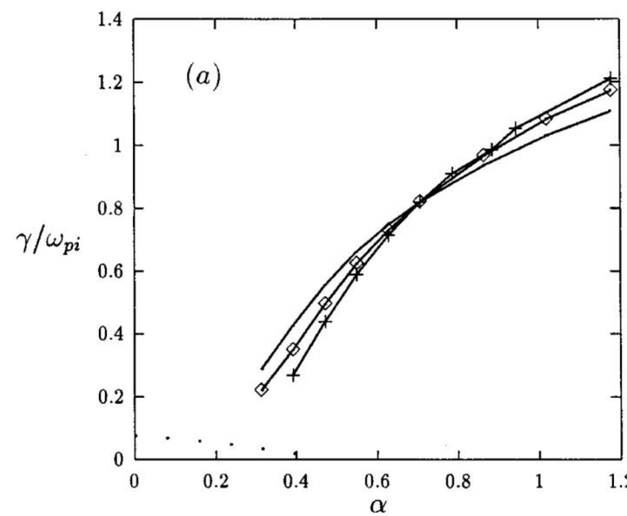

J.Q. Dong, L. Chen, F. Zonca, Nucl. Fusion, 39, 1041 (1999).

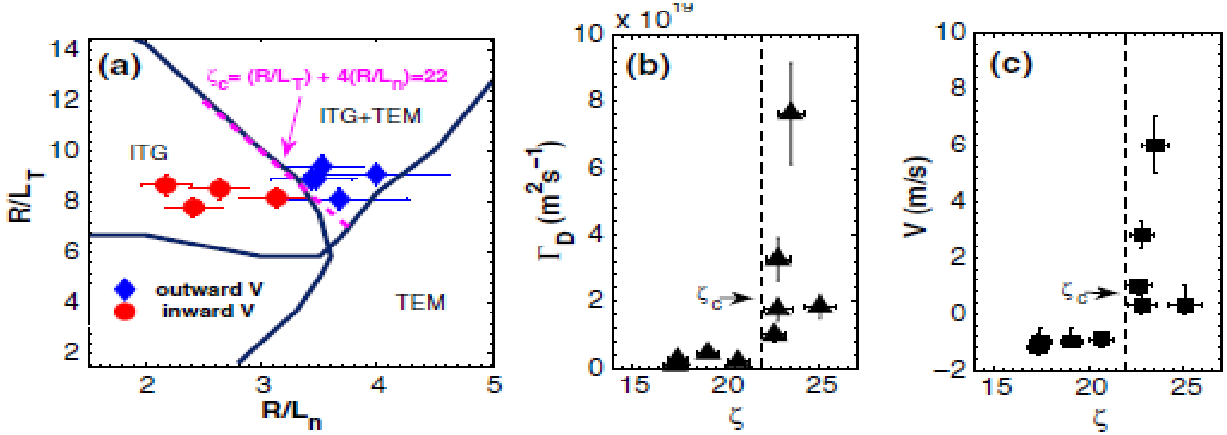

W.L. Zhong et al., PRL 111, 205001 (2013).

FIG. 6 (color online). (a) Turbulence stability diagram with QUALIKIZ model. The ITG-TEM boundary is fitted with the line of $\zeta_c = R/L_T + 4(R/L_n) = 22$, which is the mixed critical gradient including the electron density and temperature gradients. (b) Diffusive particle flux vs ζ. (c) Convective velocity vs ζ.

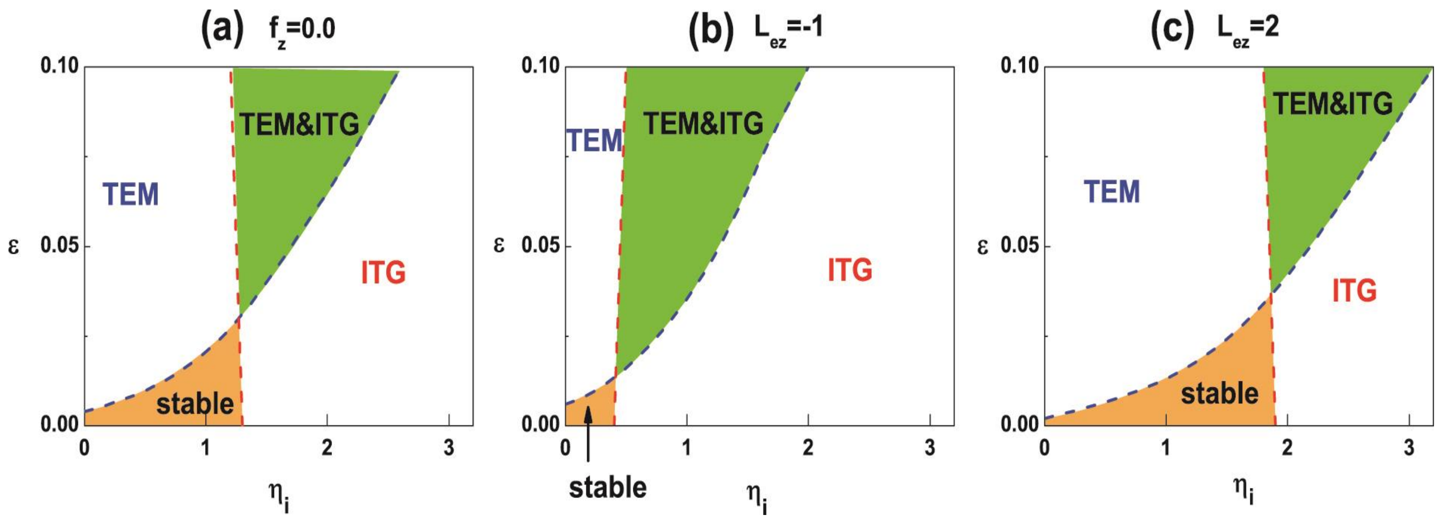

Huarong Du, Zheng-Xiong Wang, J. Q. Dong et al, PoP **21**, 052101 (2014)

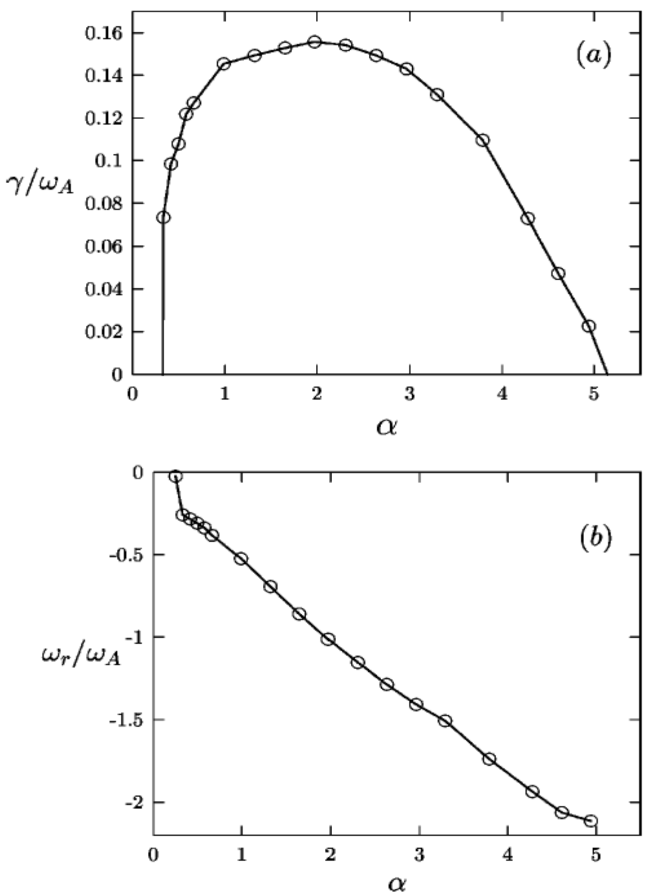

FIG. 3. The mode growth rate (a) and real frequency (b) as functions of α for $k_\theta \rho_s = 0.33$, $\eta_i = \eta_e = 1.0$, $q = 1.2$, $\epsilon_n = 0.175$, $\tau_i = 1$, $\hat{s} = 0.2$.

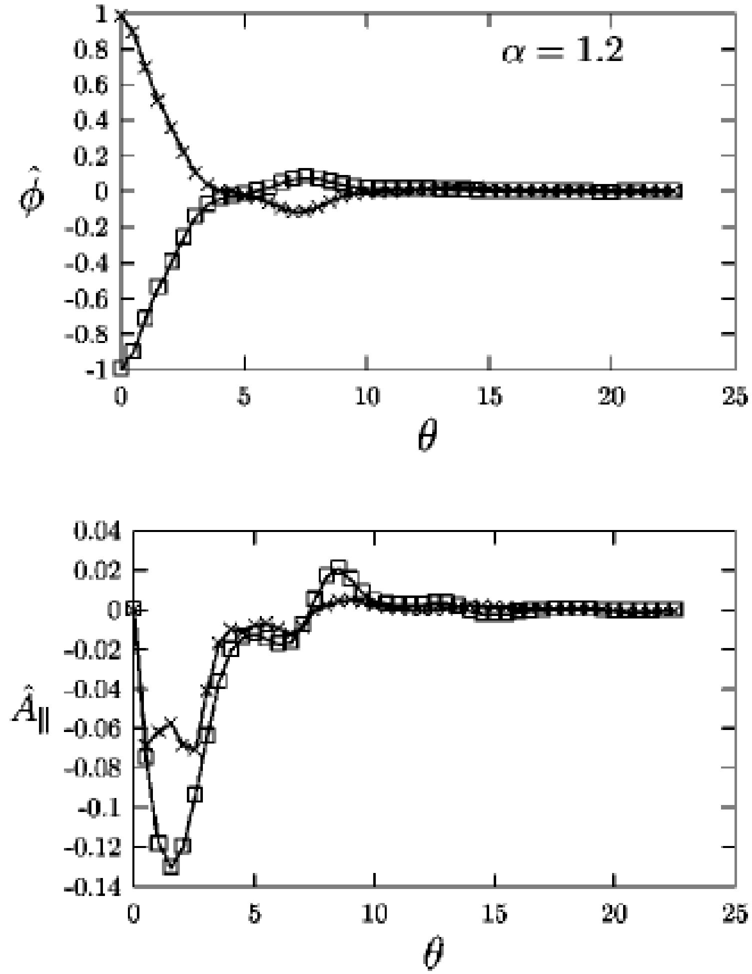

$$\alpha = \frac{q^2 \beta_i}{\epsilon_n}[(1+\eta_i) + \tau_i(1+\eta_e)] = \frac{q^2 \beta_i}{\epsilon_n}(1+\tau_i)(1+\eta_i),$$

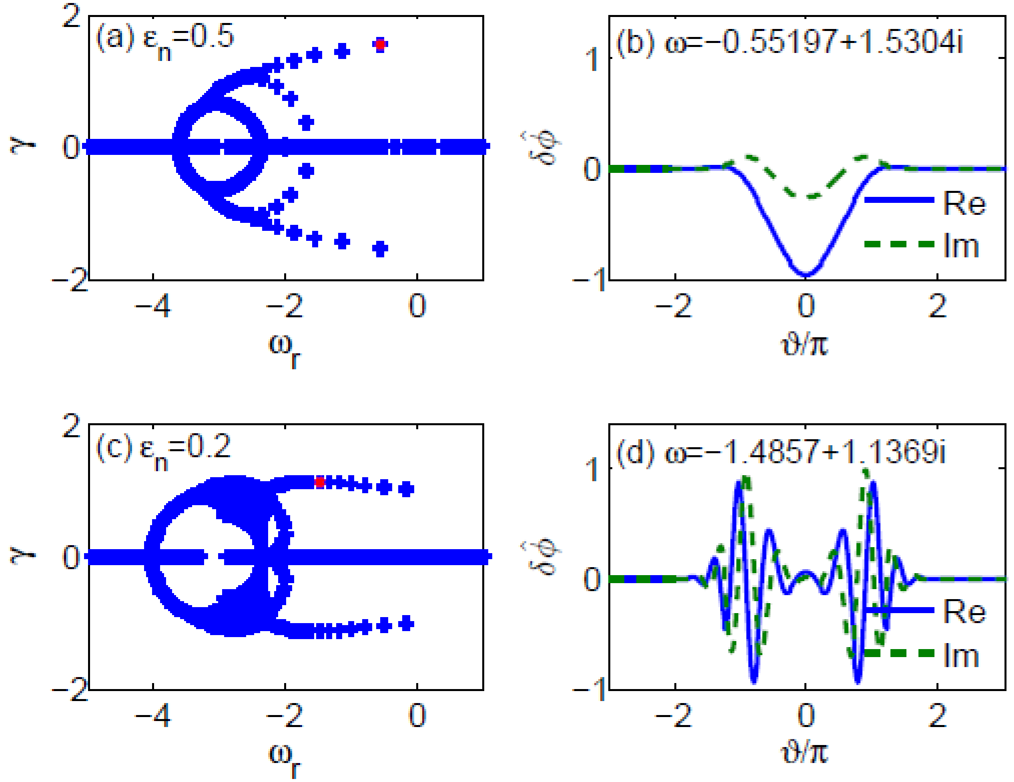

FIG. 5: In Eq.(2), series solutions exist. For weak gradient ($\epsilon_n = 0.5$), the most unstable solution (red 'x') is the ground state (a&b), which is the conventional ballooning structure. For strong gradient ($\epsilon_n = 0.2$), the most unstable solution (red 'x') is not the ground state (c&d), which represents the unconventional ballooning structure.

Xie & Xiao, PHYSICS OF PLASMAS 22, 090703 (2015)

Stabilizing factors

1） magnetic shear： related to Landau damping；

2） finite Larmore radius；

3） finite beta；

4） perpendicular velocity shear;

Destabilizing factors

1) Ion (electron) temperature gradient

2) Density gradient

3) trapped electrons

4) parallel velocity shear

5) finite beta

Outline

1. Introduction
2. Instabilities
3. **Turbulence and Zonal Flow**
4. Transport
5. Summary

(1) Turbulence

1)Reynolds number and fluid turbulence: $R = \frac{LV}{\nu}$

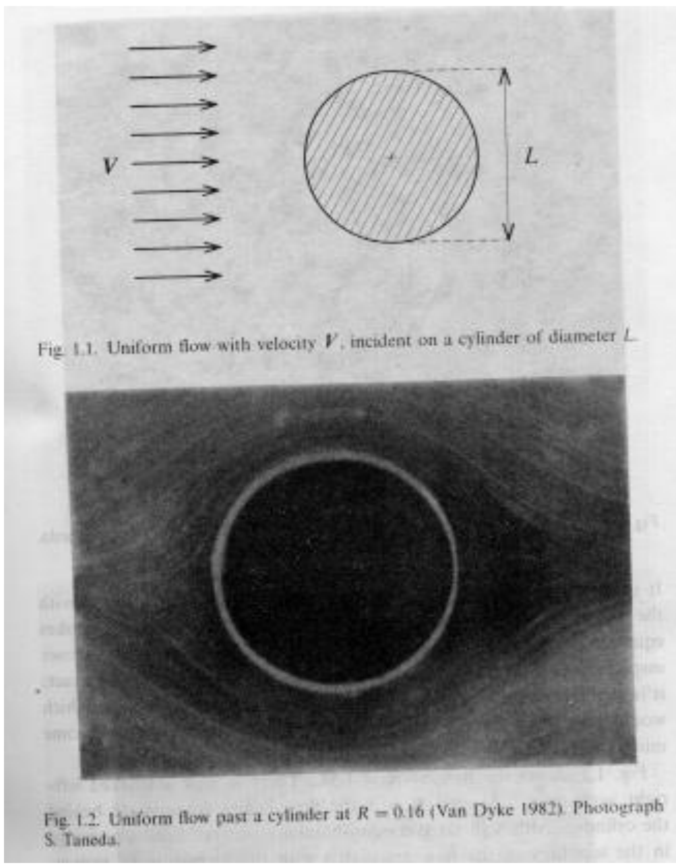

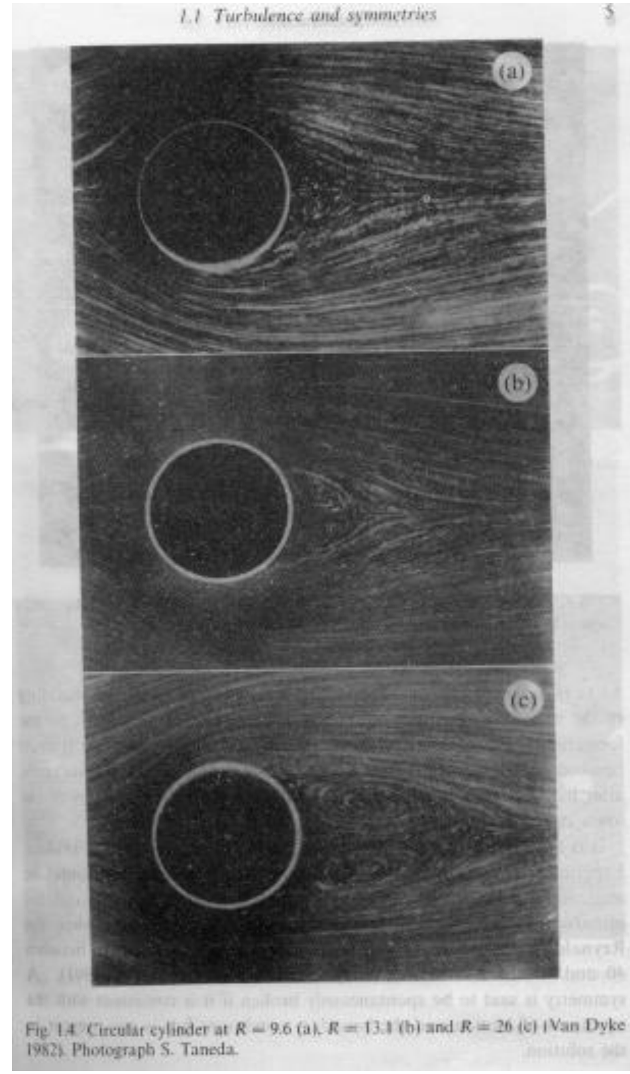

A First course in Turbulence, H. Tennekes and J.L. Lumley, MIT Press, 1973

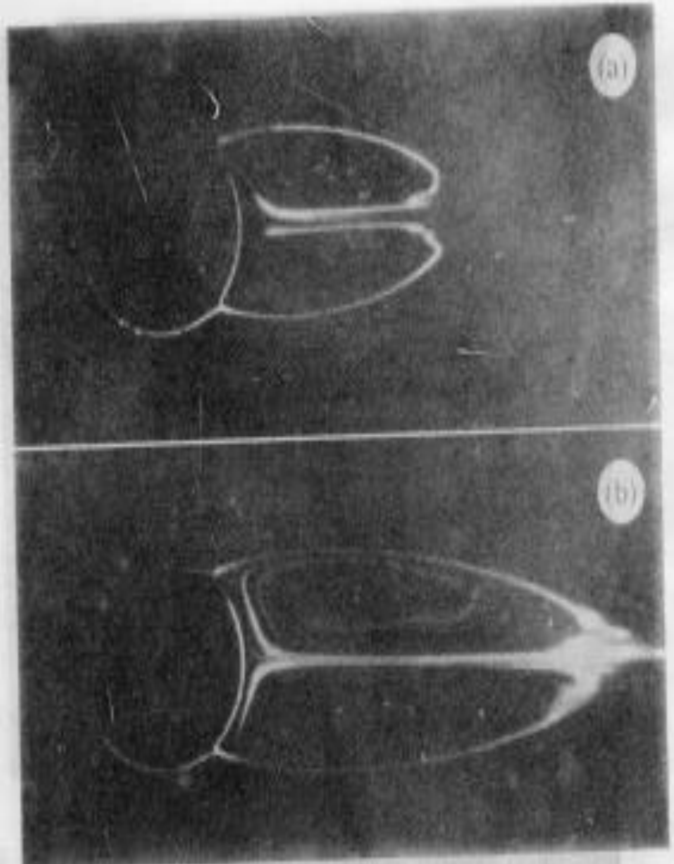

Fig. 1.5. Circular cylinder at $R = 28.4$ (a) and $R = 41.0$ (b) (Van Dyke 1982). Photograph S. Taneda.

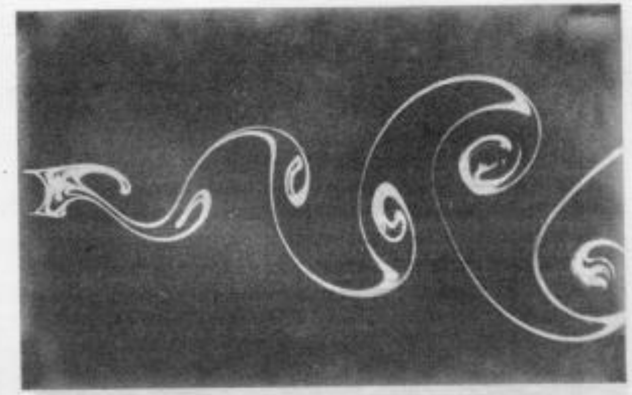

Fig. 1.6. Kármán vortex street behind a circular cylinder at $R = 140$ (Van Dyke 1982). Photograph S. Taneda.

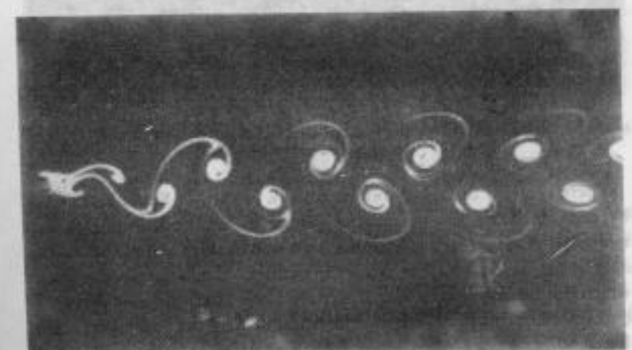

Fig. 1.7. Kármán vortex street behind a circular cylinder at $R = 105$ (Van Dyke 1982). Photograph S. Taneda.

2) Basic characteristics of turbulence: i)randomness，
ii) diffusive，iii）large Reynolds number，vi）3D，v) dissipative
vi）continuous spectra， vii）turbulence is a kind of flow

3)Plasma turbulence（micro-turbulence）

i） Nonlinear development of electrostatic or electromagnetic instabilities，

ii） Electric and magnetic perturbations are important characteristics of plasma turbulence, and the differences from fluid turbulence.

iii） Examples

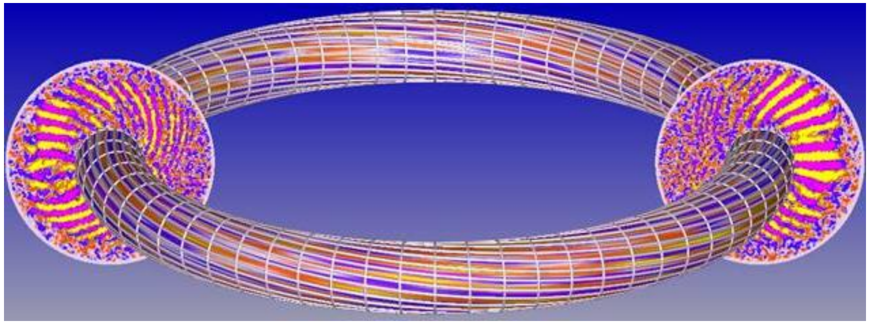

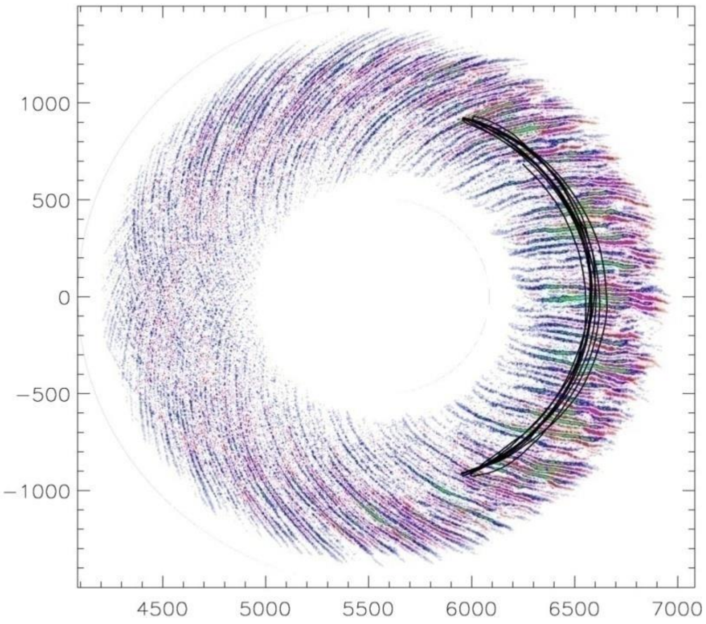

The theory of Plasma Turbulence, V.N. Tsytovich, Pergamon Press Ltd, 1972.

4) Main approaches of investigation

Computer simulation:

i）fluid/gyro-fluid (BOUT erc.);
ii）kinetic;
(i) Vlasov equation(Gyro,GS2);
(ii)particle simulation (GTC,GTS) full-f, δ f;

Weak turbulence theory: the period of linear perturbation is much shorter than the time scale of nonlinear development, may use small parameter expansion,

$$\frac{1}{\omega\tau} << 1, \quad \frac{\gamma}{\omega} << 1$$

Strong turbulence theory: perturbations and equilibrium quantities are comparable and small parameter expansion cannot be used;

Quasi-linear theory: obtaining perturbations from linear equations and substituting into nonlinear expressions, can do some qualitative analyses but cannot give quantitative results.

Particle-in-Cell Simulation of Plasma

- Electrostatic Vlasov-Poisson system in (**x**,**v**) 6D phase space

$$[\frac{\partial}{\partial t}+\mathbf{v}\cdot\frac{\partial}{\partial \mathbf{x}}+\frac{q}{m}(-\nabla\phi+\frac{1}{c}\mathbf{v}\times\mathbf{B})\cdot\frac{\partial}{\partial \mathbf{v}}]F=0$$

$$\nabla^2\phi=-4\pi e\int(F_i-F_e)d\mathbf{v}$$

- Particle-in-cell (PIC) simulation: solve Vlasov Eq. in Lagrangian coordinates
  - Monte-Carlo sampling of phase space

$$\dot{\mathbf{x}}=\mathbf{v}$$

$$\dot{\mathbf{v}}=\frac{q}{m}(-\nabla\phi+\frac{1}{c}\mathbf{v}\times\mathbf{B})$$

- Continuum simulation: solve Vlasov Eq. in Eulerian coordinates
  - Velocity grids
- Semi-Lagrangian: use velocity grids, follow particle orbits

Langmuir probe arrays

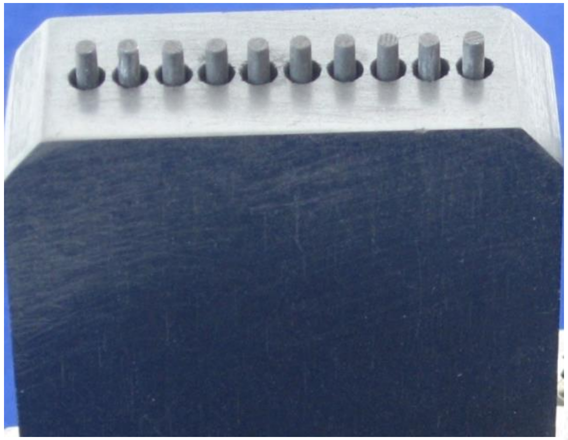

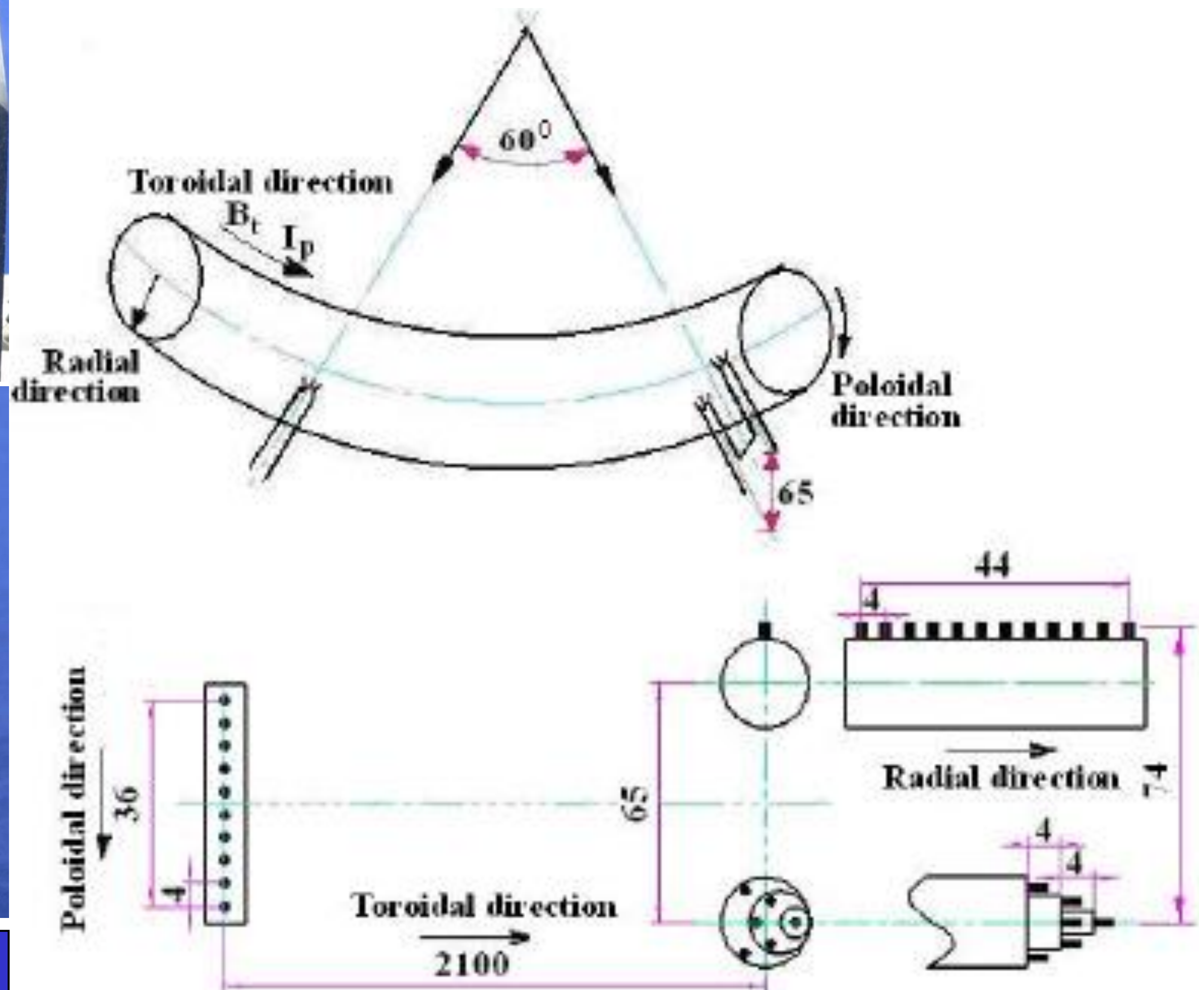

Sampling rate = 1 MHz

Physics quantities to describe turbulence

5) Wave vector-frequency power spectrum $S(k, f)$
from two fluctuation signals $\tilde{x}(t)$ and $\tilde{y}(t)$,
after FFT we get Signal spectra $X^j(f)$ and $Y^j(f)$,
by ensemble average we get Auto-power spectrum
$P^j_{XX} =< X^j(f)X^{j*}(f) >, P^j_{YY} =< Y^j(f)Y^{j*}(f) >$.
and Cross-power spectrum
$P^j_{XY} =< X^j(f)Y^{j*}(f) >$.

Local wave vector

$$k^j(f) = \frac{\theta^j(f)}{\Delta d}$$

Local wave vector frequency spectrum

$$S(k, f) = \frac{1}{M} \sum_{j=1}^{M} I_{0,\delta k}[k - k^j(f)] P^j_{XY}$$

where M is the number of samples, and

$$I_{0,\delta k}(x) = \begin{cases} 1 \ (-\Delta k < x > \Delta k) \\ 0 \ (\text{otherwise}) \end{cases}$$

Conditional power spectrum

$$S(k|f) = \frac{S(k,f)}{S(f)},$$

where

$$S(f) = \sum_k S(k, f).$$

Statistical dispersion relation

$$\bar{k}(f) = \sum kS(k|f)$$

Averaged wave vector

$$< k >= \sum_f \bar{k}(f)S(f)$$

Width of wave vector spectrum

$$\bar{\sigma}_k^2(f) = \sum_k [k - \bar{k}(f)]^2 S(k|f)$$

Correlation spectrum

$$\gamma_{XY}(f) = \frac{1}{M}\sum_{j=1}^{M} \frac{P_{XY}^j}{|P_{XX}^i P_{YY}^j|^{1/2}}.$$

Correlation length

$$l_c = 1/ < \bar{\sigma}_k^2(f) >^{\frac{1}{2}} .$$

Average phase velocity

$$\bar{v}_{ph} = \sum_{k,f} \frac{2\pi f}{k} S(k, f)$$

Normalized bicoherency

$$\hat{b}^2(f_3 = f_1 + f_2) = \frac{|< \varphi(f_1)\varphi(f_2)\varphi^*(f = f_1 + f_2)\rangle|^2}{<|\varphi(f_1)\varphi(f_2)|^2><|\varphi(f_3 = f_1 + f_2)|^2>}.$$

Summed bicoherency

$$\hat{b}_f{}^2 = \sum_{f=f_1+f_2}^{N} \hat{b}^2(f = f_1 + f_2)/N$$

(2) Zonal flow (ZF)

- In a toroidal plasma a zonal flow is a poloidal flow driven by turbulence, linearly stable, no direct flux drive.
- There are a turbulence-zonal flow systems.

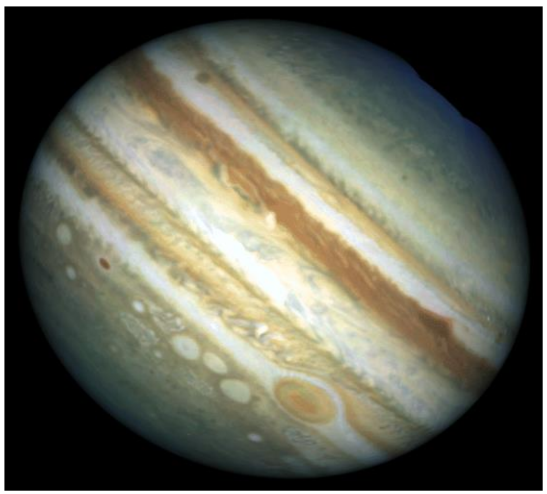

ZF in the atmosphere of Jupiter

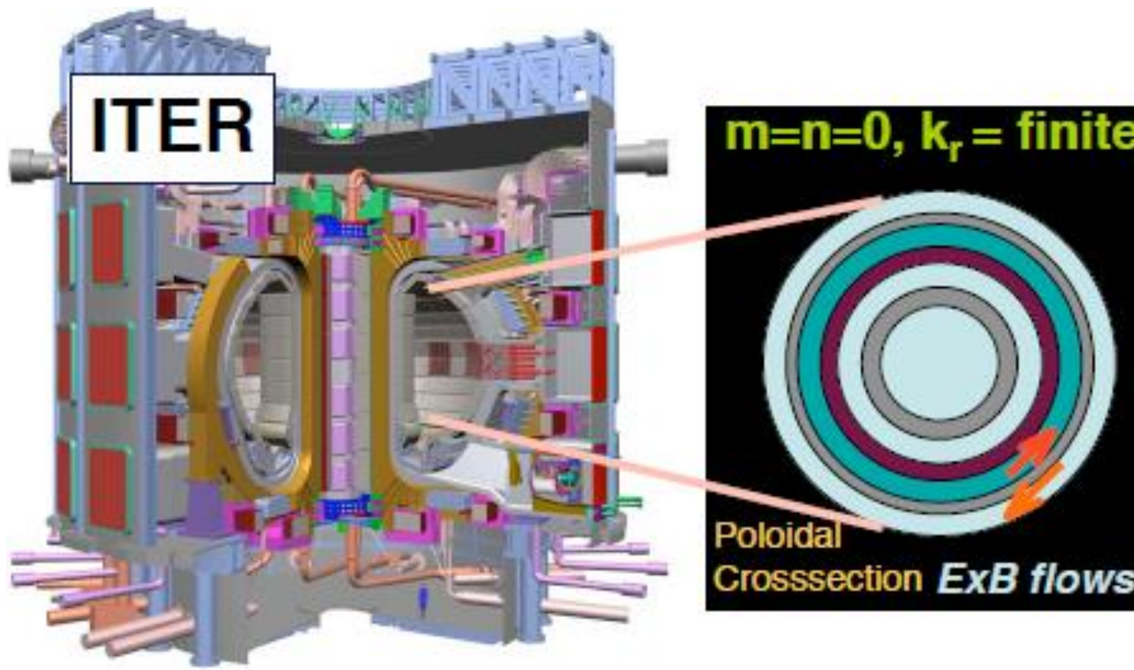

P. H. Diamond et al. PPCF 47, R35 (2005)

1) Characteristics of zonal flows

- **Electric field (or potential) fluctuations of poloidal and toroidal symmetry, finite radial wave number,**

$$n = m = 0,\ q_r \rho_i \sim 0.1$$

- **Two kinds of zonal flows**

Low frequency ZF(LFZF)

Geodesic acoustic mode (GAM)

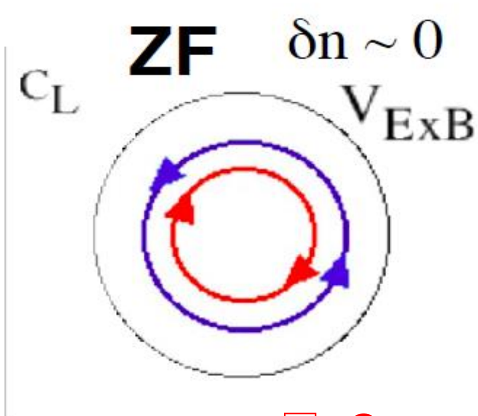

$\omega_{LFZF} \sim 0$

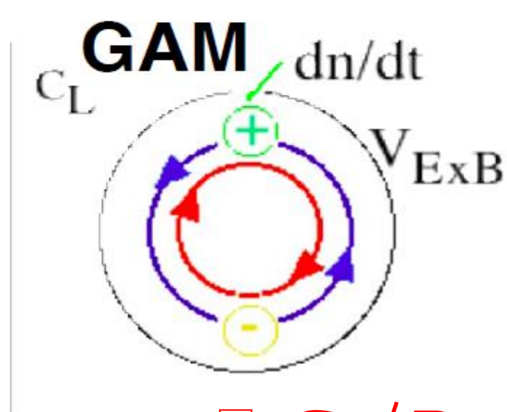

$\omega_{GAM} \sim C_S / R$

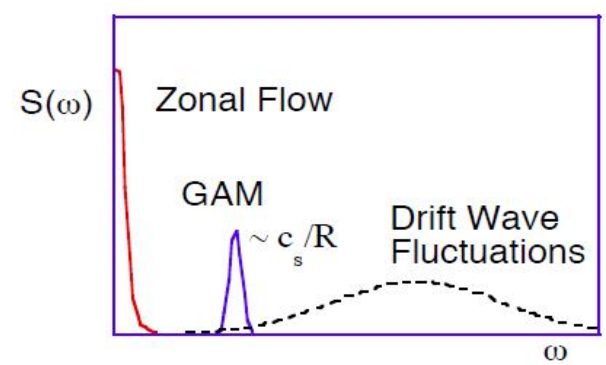

Diamond *et al*., IAEA2004

Characteristics of LFZF

- **Structure:** $\vec{E}\times\vec{B}$ **fluctuating flow**

  $m = n = 0 \quad , \quad \tilde{n}/n \sim (q_r\rho_i)^2 e\tilde{\phi}/T_e$

- **Frequency:** $\Omega_{ZF} \sim 0 \quad , \quad \Delta\Omega_{ZF} \sim \nu_{ii}$
- **Correlation time** $\varepsilon\nu_{ii}^{-1}$ or others, $\varepsilon = r/R$
- **Radial wave vector** $(\rho_i/a)^{1/2} < q_r\rho_i < 1$
- **Radial correlation length** $(a\rho_i)^{1/2}$
- **Damping rate: see the figure**
- **Amplitude** $\tilde{V}_{ZF}/V_{th,i} < 10^{-2}$

Hahm PPCF 42, A205

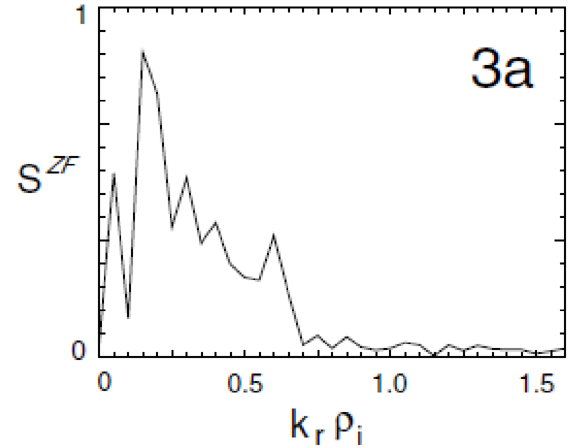

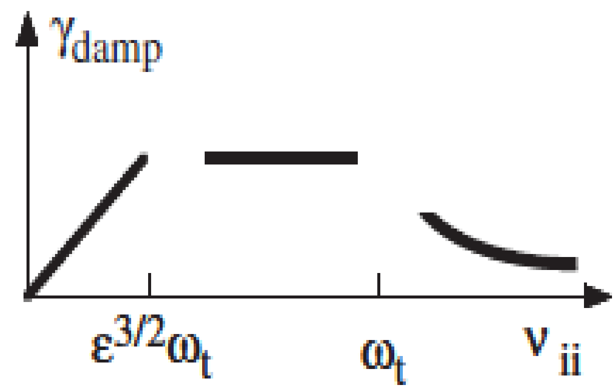

Characteristics of GAM

- **Structure:** $\vec{E} \times \vec{B}$ **fluctuating flow**

  potential $\tilde{\phi}$: $m = 0\ ,\ n = 0$

  density $\tilde{n}$: $m = 1\ ,\ n = 0\ ,\ \tilde{n}/n \sim \sin\theta \sqrt{2} q_r \rho_i \left(e\tilde{\phi}/T_e \right)$

- **Frequency** $\omega_{GAM} \sim \sqrt{2} C_s / R$
- **Correlation time** v_{ii}^{-1} or others
- **Radial wave vector and correltion length: same as LFZF**
- **Damping rate** $\gamma_{GAM} \sim \omega_{GAM} \exp\left(-q^2/2 \right)$ Landau damping

  $\gamma_{GAM} \sim 4 v_{ii}/7$ collision damping

- **Amplitude: same as LFZF**

2) Importance of ZF studies

- **ZFs modulate turbulence and reduce cross field transport;**
- **ZFs shift the critical gradient upward** $R/L_{T,C}$ **(Dimits Shift);**
- **ZFs may provide ways to control turbulence and transport, by controlling ZF damping rate (which is related to collision frequency and magnetic configuration) ;**
- **ZFs may help understanding meso-scale scale structure and its role in confinement;**
- **Possible roles in L-H transition.**

3)Formation mechanism of ZF

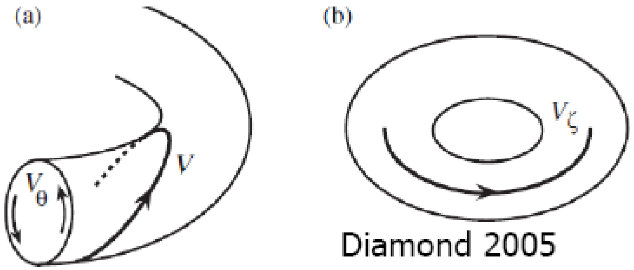

$$\nabla \cdot \left(n\tilde{V}_{E\times B}\right) = -n\tilde{V}_{E\times B}\frac{2\sin\theta}{R_0}\hat{\theta} \neq 0$$

$$\frac{\partial \tilde{n}}{\partial t} = -\nabla \cdot \left(n\tilde{V}\right) = -\nabla \cdot \left(n\tilde{V}_{E\times B}\right) - \nabla \cdot \left(n\tilde{V}_{//}\right)$$

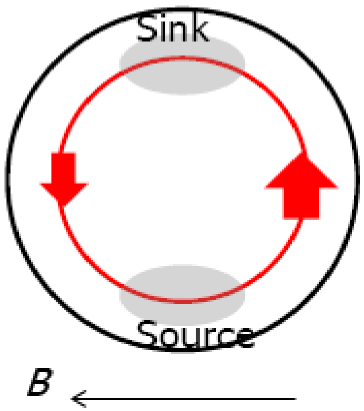

$$B = B_0/(1 + r\cos\theta/R_0)$$

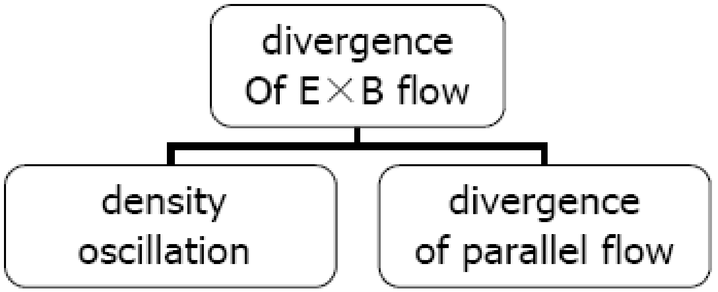

- **Stationary ZF: the compression is fully compensated by a toroidal return flow** $V_\varphi/V_{E\times B} = -2q\cos\theta$
- **Geodesic acoustic mode: mainly by a temporal oscillation of density, and only a small part by ion sound wave /parallel transit flow**

GAM: the fluid picture

$$\frac{\partial \tilde{\rho}}{\partial t} = \nabla \cdot \left(-\rho \frac{\tilde{E}}{B} \right)$$

divergence of fluctuating E*B flow
→ density fluctuation

$$\tilde{\rho} \sim \tilde{E} \sin\theta / \omega B R_0 \sim O(k_x \rho_i) \frac{e\tilde{\phi}}{T}$$

$$\frac{\nabla \tilde{p}}{\nabla \tilde{\rho}} = \frac{\gamma p}{\rho} = c_s^2$$

density fluctuation
→pressure fluctuation
(adiabatic or isothermal)

$$J_\perp = \frac{1}{B} \frac{\partial}{\partial t} \left(-\rho \frac{\tilde{E}}{B} \right) + \frac{\nabla_\perp \tilde{p}}{B}$$

diamagnetic current
due to pressure fluctuation
+polarization current
due to time-varying electric field

$$\langle J_\perp \rangle_\Psi = 0$$

Quasi-neutrality condition
→ radial current balance

⇒

$$\omega^2 = \frac{2c_s^2}{R_0^2}$$

GAM: the fluid picture (ctd.)

$$\frac{\partial \tilde{\rho}}{\partial t} = \nabla \cdot \left(-\rho \frac{\tilde{E}}{B} \right) + \nabla \cdot \left(\rho \tilde{V}_{//} \right)$$

divergence of fluctuating E*B flow
→ density fluctuation

$$\tilde{\rho} \sim \tilde{E} \sin\theta / \omega B R_0 \sim O(k_x \rho_i) \frac{e\tilde{\phi}}{T}$$

$$\frac{\nabla \tilde{p}}{\nabla \tilde{\rho}} = \frac{\gamma p}{\rho} = c_s^2$$

density fluctuation
→pressure fluctuation
(adiabatic or isothermal)

$$J_\perp = \frac{1}{B} \frac{\partial}{\partial t} \left(-\rho \frac{\tilde{E}}{B} \right) + \frac{\nabla_\perp \tilde{p}}{B}$$

diamagnetic current
due to pressure fluctuation
+polarization current
due to time-varying electric field

$$\left\langle J_\perp \right\rangle_\Psi = 0$$

Quasi-neutrality condition
→ radial current balance

$$\rho \frac{\partial}{\partial t} \tilde{V}_{//} = -\nabla_{//} \tilde{p}$$

→

$$\omega^2 = \frac{2 c_s^2}{R_0^2} \left(1 + \frac{1}{2 q^2} \right)$$

Winsor 196

Kinetic theory of GAM: model

- Assume a rigid constant on a magnetic surface (m=n=0)

$$\tilde{\phi} = \sum_{\omega,k} \hat{\phi} \exp\left[ik(r - r_0) - i\omega t\right]$$

- Quasi-neutrality condition is the same $\nabla \cdot \mathbf{j} \sim \langle j_r \rangle = 0$

  but difference between particle drifts and fluid drift

$$\int R d\theta d^3 v \left[(\omega_d \sin\theta)\hat{f} - \left(\frac{\omega}{\Omega}\frac{k\hat{\phi}}{B} g_{FLR}\right) F_0 \right] = 0$$

radial component of magnetic curvature drift

polarization drift (lower order)

- The perturbed distribution function given by the gyro-kinetic equation

$$\hat{f} = -qF_0\hat{\phi}/T + \hat{h}J_0, \quad \left(\omega - \omega_d \sin\theta + i\omega_t \frac{\partial}{\partial\theta}\right)\hat{h} = \frac{qF_0}{T}\omega J_0 \hat{\phi}$$

$$J_0 = J_0(k\rho), \quad \rho = v_\perp/\Omega_0, \quad \omega_t = v_{//}/(qR_0), \quad \omega_d = k\left[\left(2v_{//}^2 + v_\perp^2\right)/(2\Omega_0 R_0)\right]$$

Kinetic theory of GAM: drift-kinetic limit

$$\int_L \frac{d^3v \exp(-v^2)}{\pi^{3/2}} J_0^2(kv_\perp) \sum_{n=1}^{+\infty} J_n^2\left(kq\frac{v_{//}^2 + v_\perp^2/2}{v_{//}}\right)\left(\frac{v_{//}}{\zeta/n - v_{//}} + \frac{-v_{//}}{\zeta/n + v_{//}}\right) = \frac{k^2}{2} g_{FLR}$$

$k \rightarrow 0$, the lowest order

$$\frac{1}{q^2} + \frac{1}{2} - \frac{1}{2\zeta^2} + \left(\zeta^2 + 1 + \frac{1}{2\zeta^2}\right)[1 + \zeta Z(\zeta)] = 0$$

For conventional GAM $\zeta \equiv qR\omega/v_{ti} \sim q >> 1$

$$\frac{1}{q^2} - \frac{7}{4\zeta^2} - \frac{23}{8\zeta^4} + i\pi^{1/2}\zeta^3 e^{-\zeta^2} = 0$$

Weakly damped $\gamma << \omega_r$

$$\omega_{GAM}^2 = \frac{7}{4}\frac{v_{ti}^2}{R^2}\left(1 + \frac{46}{49q^2}\right)$$

$$\gamma_{GAM} = -0.52\frac{v_{ti}}{R} q^5 \exp\left(-\frac{7q^2}{4}\right)$$

Gao 2006

Effects of electron dynamics on GAM damping rate

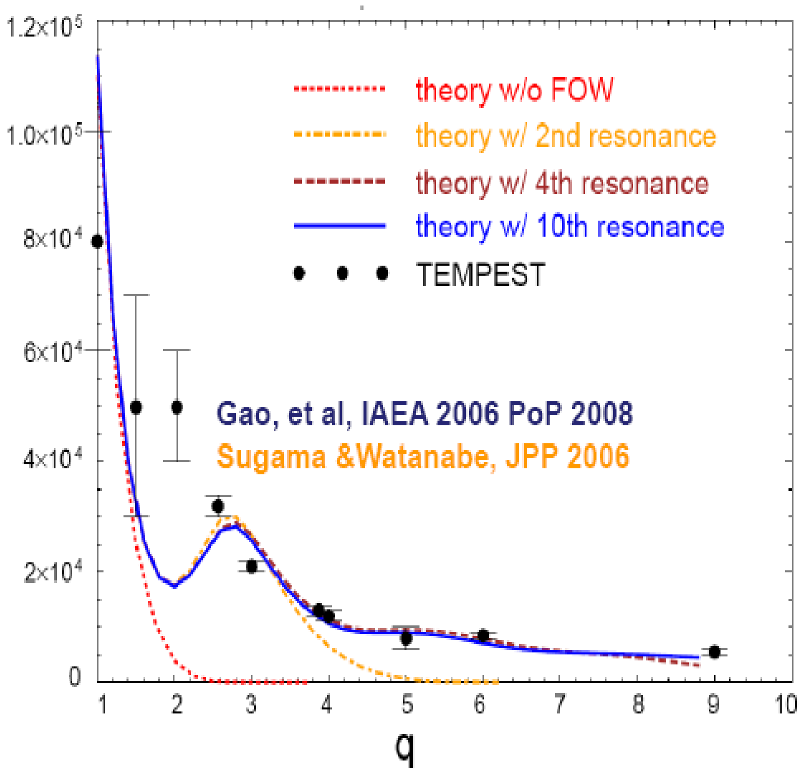

Xu 2008

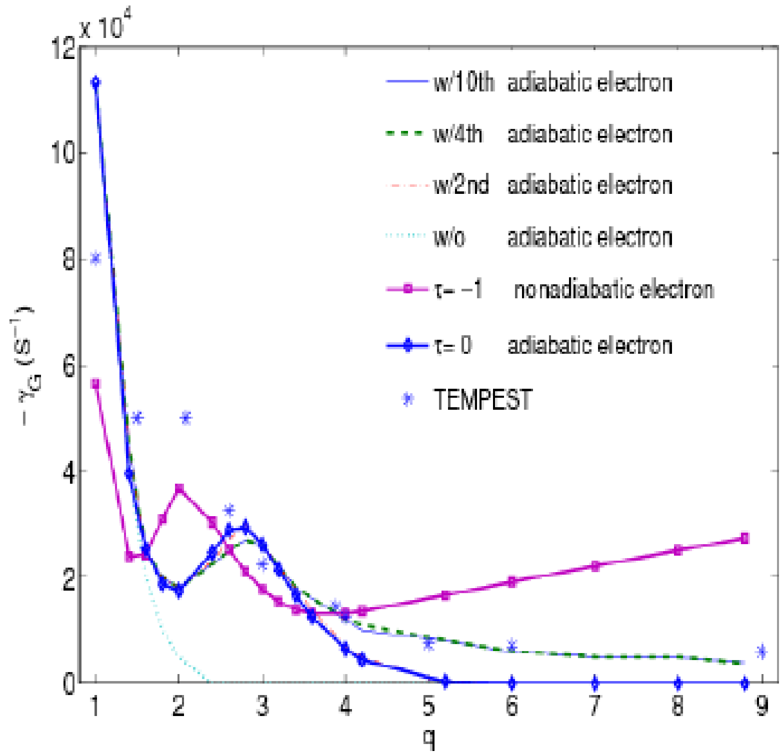

Wang PoP 18，052506（2011）.

4) Effects on zonal flow on turbulence

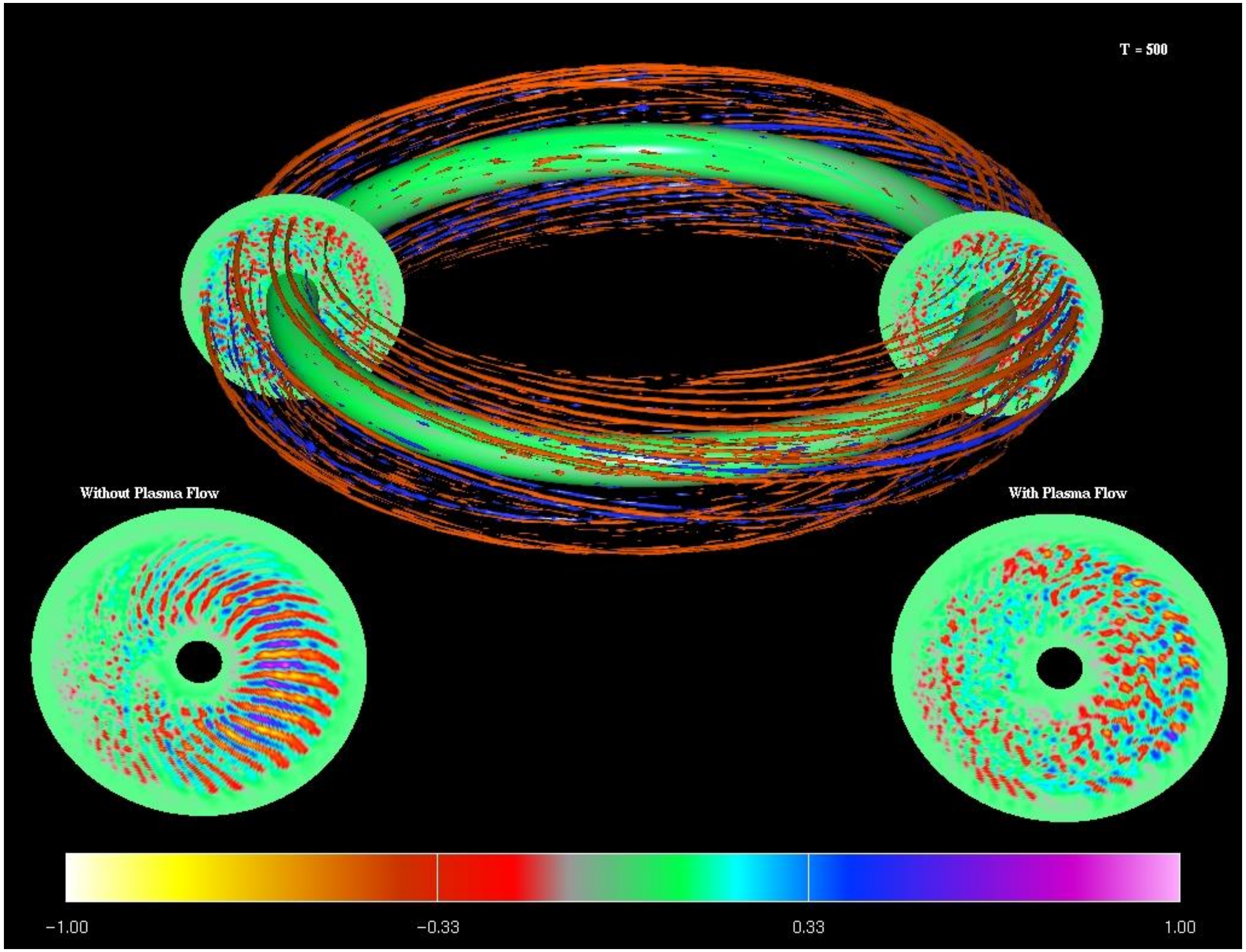

Lin et al., Science 281, 1835 (1998)

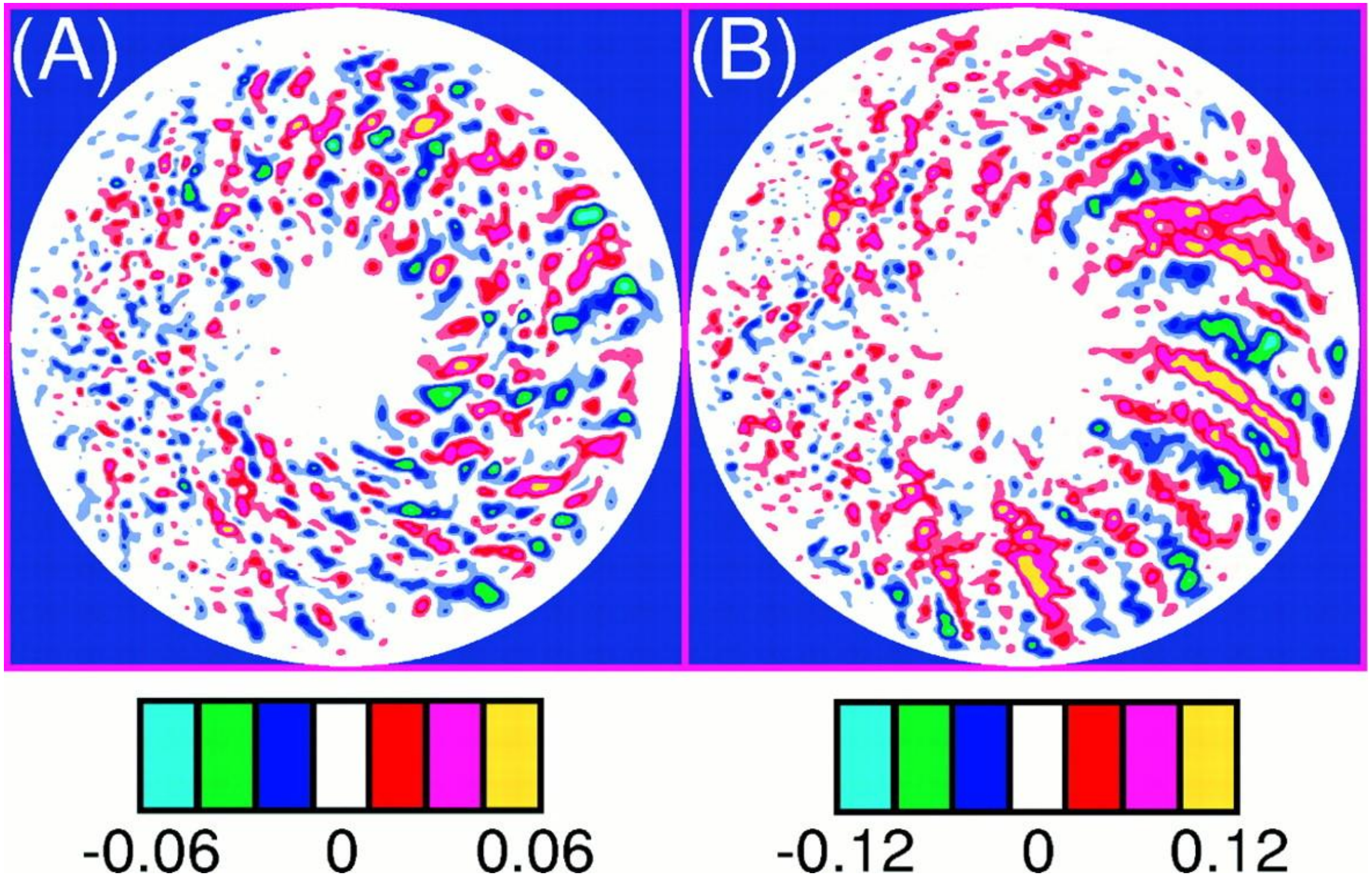

Gyrokinetic Simulation of Turbulence Driven Geodesic Modes in Edge Plasmas of HL-2A Tokamak

Feng Liu, Z. Lin, J. Q. Dong, K. J. Zhao, Physics of Plasmas **17**, 112318 (2010).

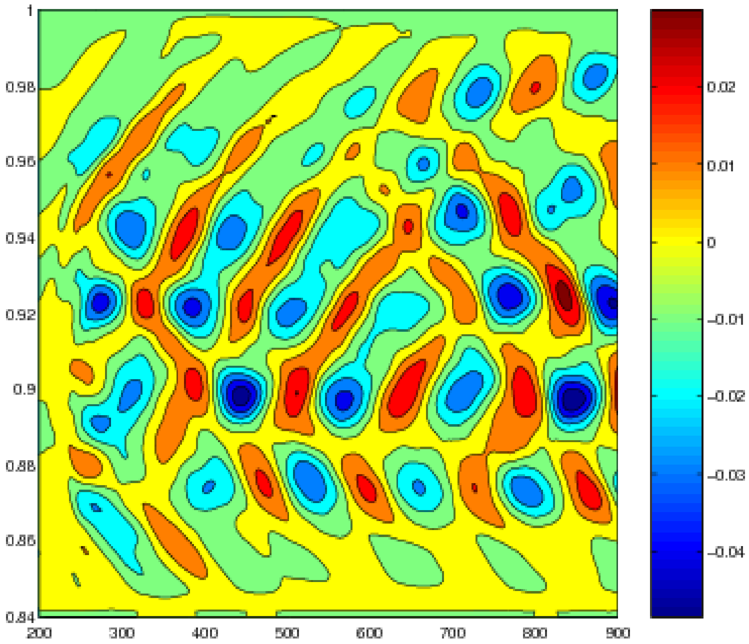

GAM propagates both inward and outward but dominated outward.

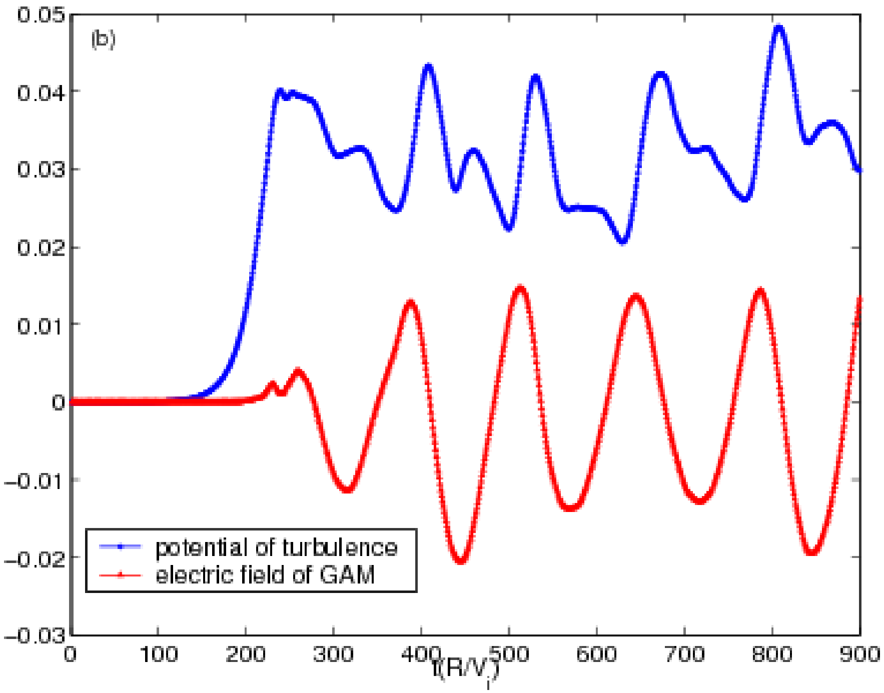

Time evolution of turbulence intensity (blue line) and zonal flow electric field (red line) .

5)Experimental data analysis

Auto- power spectrum

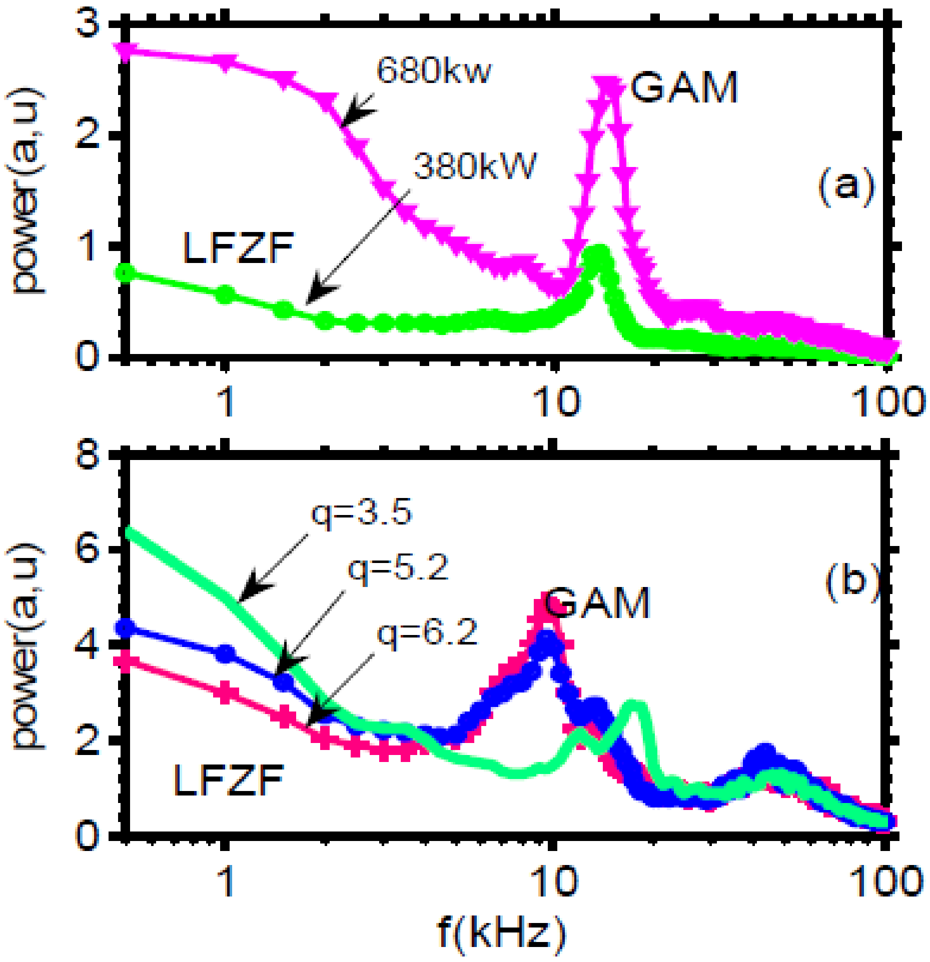

- **Auto-power spectra of floating potential, showing LFZF and GAM.**
- **Intensities if LFZF and GAM increase with ECRH power.**
- **Intensity of LFZF (GAM) decreases (increases) with safety factor q increase.**

Cross power spectrum

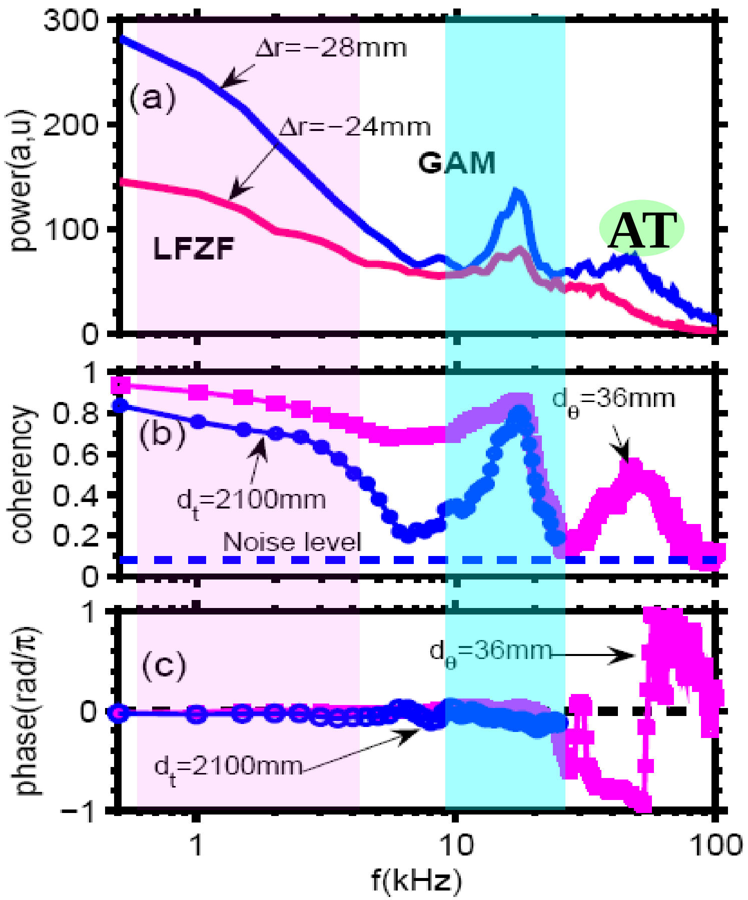

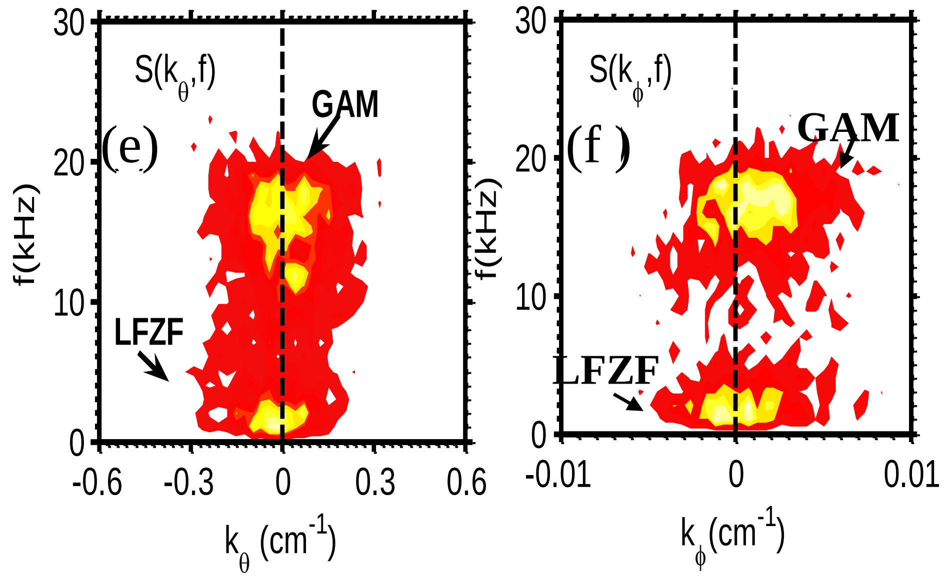

The poloidal and toroidal symmetries, i.e, *m=0,n=0* were measured, simultaneously, for LFZF and GAM.

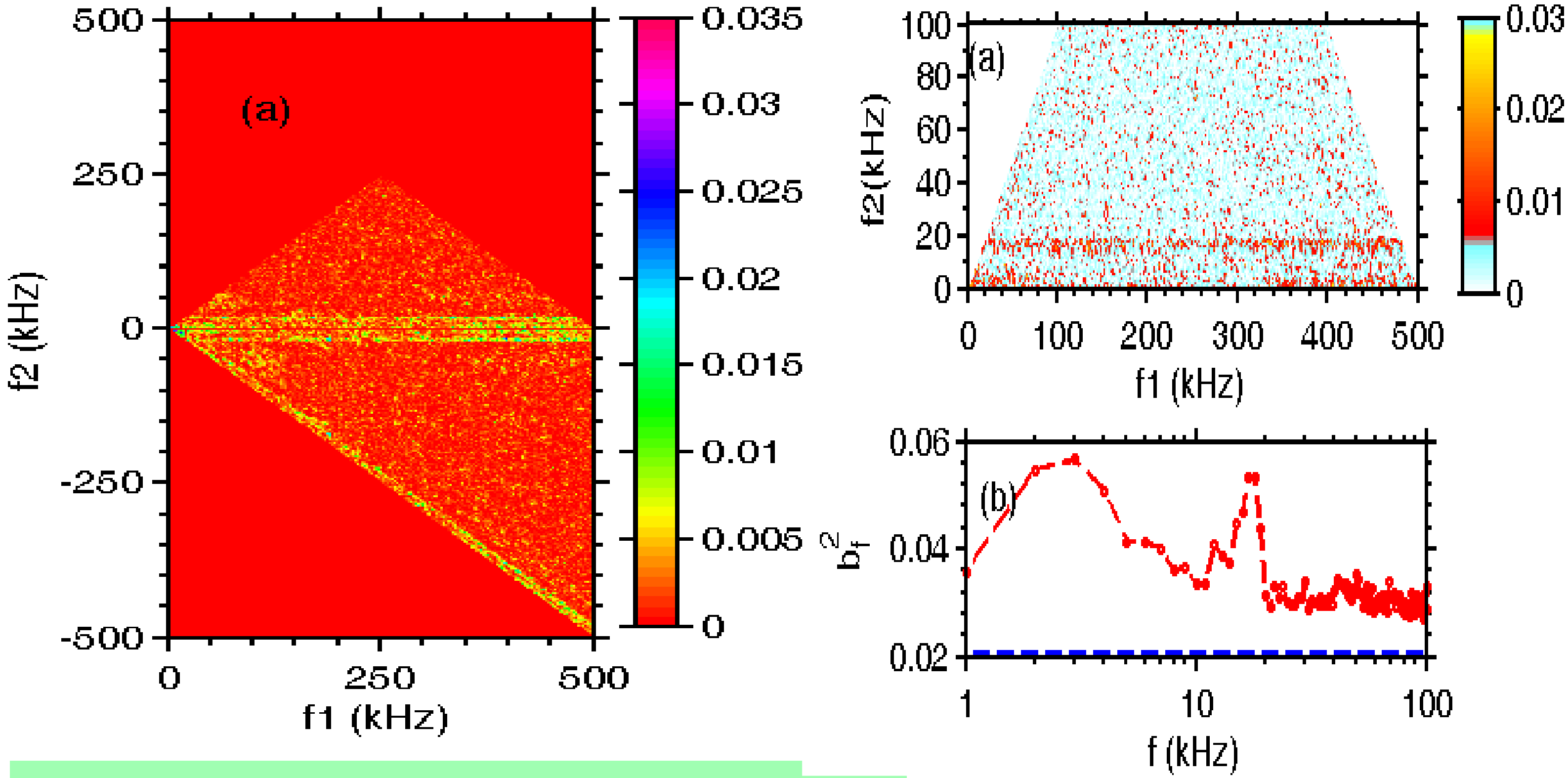

(a) Squared auto-bicoherency contour,
(b) Zoomed-in part
(c) summed auto-bicoherency.

$$\hat{b}_f^{\ 2} = \sum_{f=f_1+f_2}^{N} \hat{b}^2(f = f_1 + f_2)/N$$

$$\hat{b}^2(f = f_1 + f_2) = \frac{<\varphi(f_1)\varphi(f_2)\varphi^*(f = f_1 + f_2)\rangle}{[<|\varphi(f_1)\varphi(f_2)|^2><|\varphi(f = f_1 + f_2)|^2>]}$$

Finite radial wave number

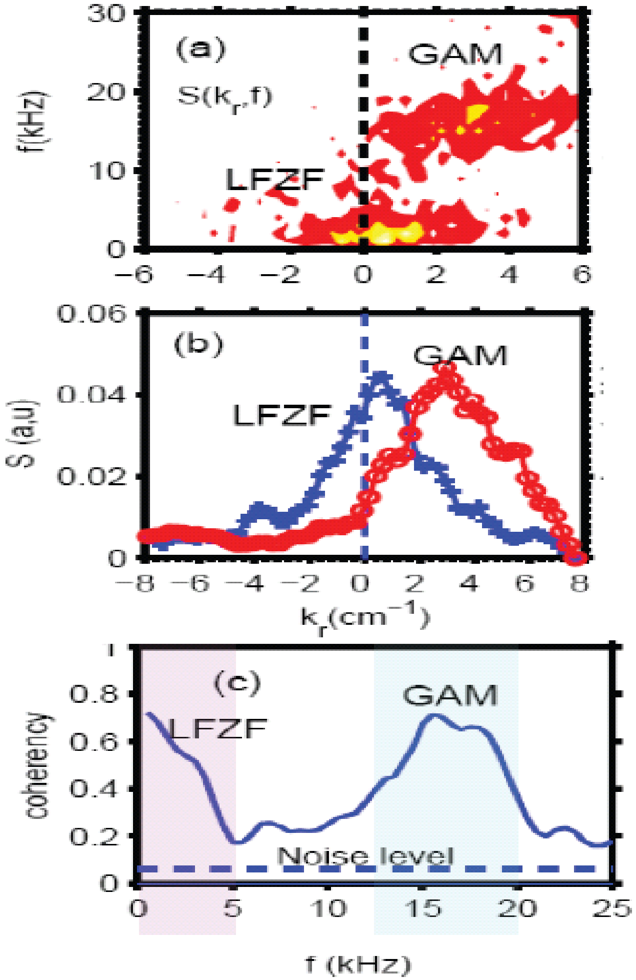

(a) Radial wave vector-frequency spectrum of potential fluctuations, and

(b) radial wave vector spectra for the LFZF and GAM;

c) Radial coherency spectrum.

- K_r=0.6cm^{-1}, Δk_r =3.7cm^{-1} for the LFZF
- K_r=3.8cm^{-1}, Δk_r =3.8cm^{-1} for the GAM

First observation of oroidal mode number (*n~0*)

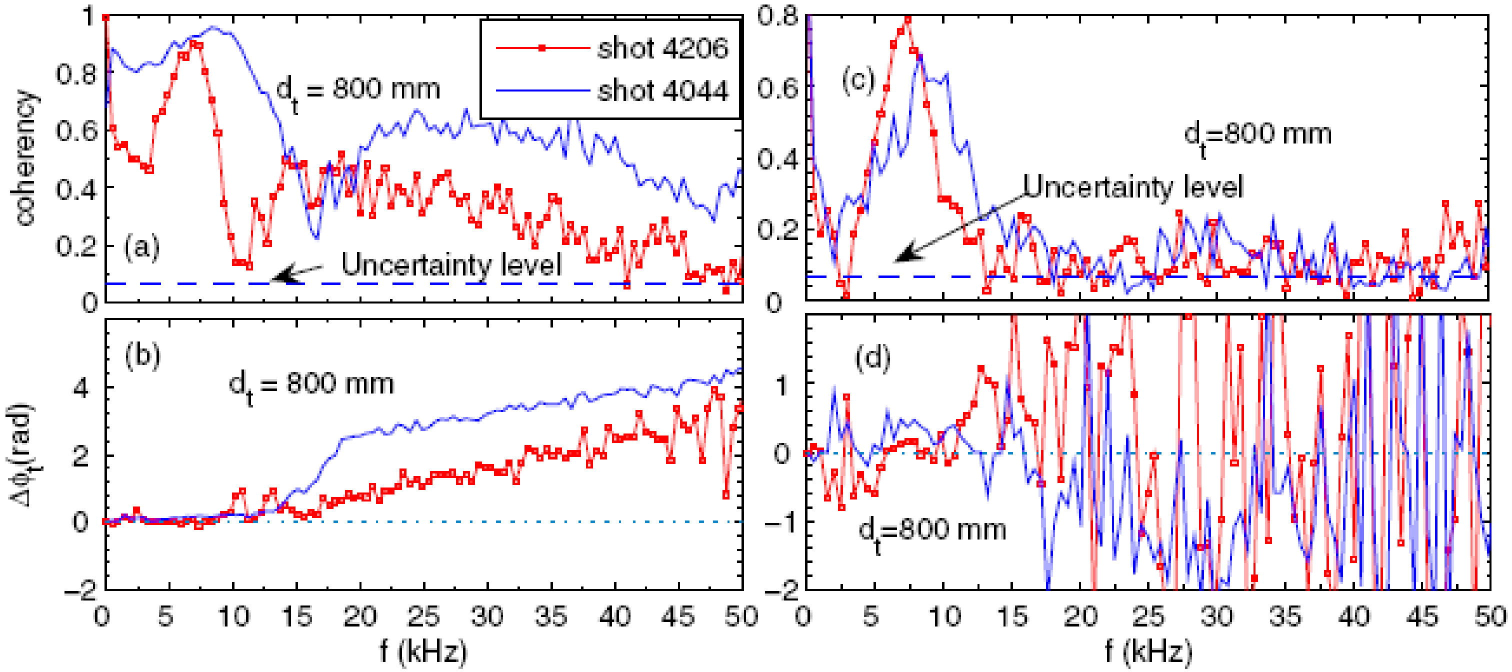

- **The toroidal mode numbers are *n~0* . GAM is uniform at a flux surface but the AT is localized to and aligned along a magnetic filed line. (a)(b) along magnetic field line, (c)(d) deviating from a magnetic filed line.** **(K.J. Zhao, T. Lan, J.Q. Dong et al., Phys. Rev. Lett. 96 (25) 255004 (2006).)**

Identification of poloidal mode number (*m<1*)

- The poloidal coherencies (a), the phase differences *(b)* and the poloidal wave vector spectra (c).
- The poloidal mode numbers are less than 1.
- The ambient turbulences (ATs) propagate in electron diamagnetic drift direction.

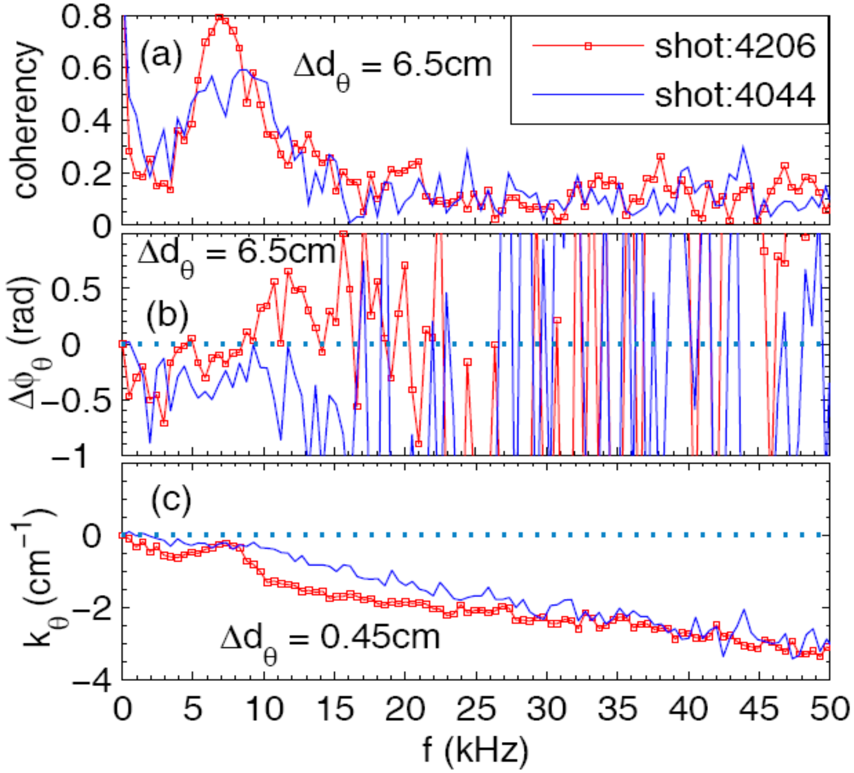

- The general dispersion relations, straight lines without offsets , for the ATs and deviations from it in the GAM frequency region are clearly shown.

Radial dependence of zonal flow intensity

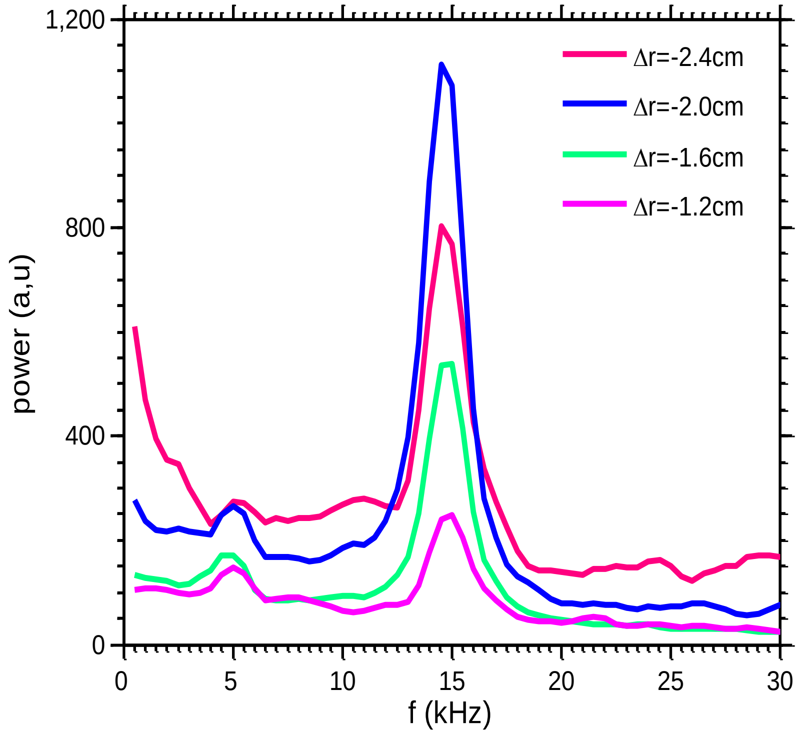

Home work：1，What is a zonal flow? How many kinds ZFs there are?
What are the differences between them?
2，Is a zonal flow an eigenmomode? Why?
3. Is it possible to have a zonal magnetic field from turbulence?

Outline

Quasi-linear Analysis of momentum transport

J.Q. Dong, W. Horton et al., Phys. Plasmas 1, 3250 (1994).

$$\frac{d^2\phi(x)}{dx^2} - b_s\phi(x) + \frac{1-\hat{\omega}}{\hat{\omega}+K}\phi(x) + \left(\frac{s^2x^2}{\hat{\omega}^2} - \frac{\hat{v}'_{0\parallel}sx}{(\hat{\omega}+K)\hat{\omega}}\right)\phi(x) = 0, \qquad (1)$$

where $b_s = k_y^2\rho_s^2$, $\hat{\omega} = \omega/\omega_{*e}$, $K = (1+\eta_i)/\tau$, $\tau = T_e/T_i$, $\eta_i = d\ln T_i/d\ln n$, $\omega_{*e} = k_y\rho_s c_s/L_n$ is the electron diamagnetic frequency, x is normalized to $\rho_s = c_s/\Omega - (T_e/m_i)^{1/2}/\Omega = c(m_iT_e)^{1/2}/eB$, Ω is the ion gyrofrequency, $\hat{v}'_{0\parallel} = L_n\, dv_\parallel/c_s\, dx$, and $s = L_n/L_s$, with L_n being the density gradient scale length. Here T_e and T_i are the electron and ion temperature, respectively. Equation (1) is valid in the hydrodynamic-like limit and the full kinetic equation is also given in Ref. 4.

Eigen-value and eigen-function

$$\left(-b_s+\frac{1-\hat{\omega}}{\hat{\omega}+K}-\frac{\hat{v}_{0\parallel}^2}{4(\hat{\omega}+K)^2}\right)\frac{\hat{\omega}}{is}=2n+1. \qquad (2)$$

The corresponding eigenfunction is

$$\phi^{(n)}(x)=\phi_0^{(n)}(\hat{\omega}/is)H_n[(is/\hat{\omega})^{1/2} \times(x+\Delta)]e^{-is(x+\Delta)^2/2\hat{\omega}}, \qquad (3)$$

where H_n is the Hermite function of order n and

$$\Delta=-\frac{\hat{v}_{0\parallel}'\hat{\omega}}{2s(\hat{\omega}+K)}. \qquad (4)$$

Potential perturbation $\tilde{\phi} = \mathrm{Re}[\Sigma_{k_y}\phi_0\phi(x)\exp(-i\omega t+ik_y y)]$.

E×B drift velocity is

$$\tilde{v}_x=-\frac{c}{B}\frac{\partial\tilde{\phi}}{\partial y}, \quad \tilde{v}_y=\frac{c}{B}\frac{\partial\tilde{\phi}}{\partial x}, \qquad (5)$$

Reynolds stress and energy flux

Define

$$\pi_{xy}(x) = \tilde{v}_x^* \tilde{v}_y + \tilde{v}_x \tilde{v}_y^* , \quad (6)$$

$$\pi_{x\parallel}(x) = \tilde{v}_x^* \tilde{v}_\parallel + \tilde{v}_x \tilde{v}_\parallel^* , \quad (7)$$

Calculated results

$$\pi_{xy} = |\phi_0|^2 \frac{c^2}{\rho_s B^2} \frac{2k_y}{s} (2x\hat{\omega}_r + \Delta\hat{\omega}^* + \Delta^*\hat{\omega}) \times e^{is[\hat{\omega}(x+\Delta^*)^2 - \hat{\omega}^*(x+\Delta)^2]/2|\hat{\omega}|^2}, \quad (8)$$

$$\pi_{x\parallel} - |\phi_0|^2 \frac{cc_s e}{BT_e} \frac{x}{s} (-2k_y\gamma) \times e^{is[\hat{\omega}(x+\Delta^*)^2 - \hat{\omega}^*(x+\Delta)^2]/2|\hat{\omega}|^2}, \quad (9)$$

For energy transport we need the radial flux $q_x(x)$ of the ion pressure fluctuation,

$$q_x(x) = \tilde{v}_x^* \tilde{p} + \tilde{v}_x \tilde{p}^* = |\phi_0|^2 \frac{P_0(1+\eta_i)c^2}{\rho_s c_s B^2} \frac{2\gamma k_y}{s^2} \times e^{is[\hat{\omega}(x+\Delta^*)^2 - \hat{\omega}^*(x+\Delta)^2]/2|\hat{\omega}|^2}, \quad (10)$$

$$\langle \pi_{xy} \rangle = \int_{-\infty}^{+\infty} (\tilde{v}_x^* \tilde{v}_y + \tilde{v}_x \tilde{v}_y^*) dx$$

$$= -|\phi_0|^2 \frac{c^2 k_y}{B^2 \rho_s} \frac{\sqrt{\pi} |\hat{\omega}|^3 K \hat{v}'_{0\|}}{s^{5/2} \gamma^{1/2} |\hat{\omega} + K|^2} e^{\gamma \hat{v}'^2_{0\|} K^2 / 4s |\hat{\omega} + K|^4}, \tag{11}$$

$$\langle \pi_{x\|} \rangle = \int_{-\infty}^{+\infty} (\tilde{v}_x^* \tilde{v}_\| + \tilde{v}_x \tilde{v}_\|^*) dx$$

$$= -|\phi_0|^2 \frac{c c_s e}{B T_e s^{5/2}} \sqrt{\pi} \frac{k_y \gamma^{1/2} |\hat{\omega}|^3 \hat{v}'_{0\|}}{|\hat{\omega} + K|^2} \times e^{\gamma \hat{v}'^2_{0\|} K^2 / 4s |\hat{\omega} + K|^4}, \tag{12}$$

and

$$\langle q_x \rangle = \int_{-\infty}^{+\infty} (\tilde{v}_x^* \tilde{p} + \tilde{v}_x \tilde{p}^*) dx$$

$$= |\phi_0|^2 \frac{P_0 (1 + \eta_i) c^2}{\rho_s c_s B^2} \frac{(\pi \gamma)^{1/2} |\hat{\omega}| k_y}{s^{5/2}} e^{\gamma \hat{v}'^2_{0\|} K^2 / 4s |\hat{\omega} + K|^4}. \tag{13}$$

The momentum transport coefficients $\mu_\perp$ and $\mu_\|$ are defined by

$$\mu_\perp = \frac{\langle \pi_{xy} \rangle}{-dv_\|/dx}$$

$$= |\phi_0|^2 \frac{c^2 k_y (\pi)^{1/2} |\hat{\omega}|^3 K L_n}{c_s B^2 \rho_s s^{5/2} \gamma^{1/2} |\omega + K|^2} e^{\gamma \hat{v}_{0\|}'^2 K^2 / 4s |\hat{\omega} + K|^4} \qquad (14)$$

and

$$\mu_\| = \frac{\langle \pi_{x\|} \rangle}{-dv_\|/dx}$$

$$= |\phi_0|^2 \frac{c e k_y (\pi)^{1/2} |\hat{\omega}|^3 L_n \gamma^{1/2}}{B T_e s^{5/2} |\hat{\omega} + K|^2} e^{\gamma \hat{v}_{0\|}'^2 K^2 / 4s |\hat{\omega} + K|^4}. \qquad (15)$$

The energy transport coefficient χ is defined as

$$\chi = \frac{\langle q_x \rangle}{-dP_0/dx}$$

$$= \frac{L_n}{P_0(1+\eta_i)} \langle \tilde{v}_x^* \tilde{p} + \tilde{v}_x \tilde{p}^* \rangle$$

$$= |\phi_0|^2 \frac{c^2 L_n |\hat{\omega}| k_y (\pi \gamma)^{1/2}}{c_s B^2 \rho_s s^{5/2}} e^{\gamma \hat{v}_{0\|}'^2 K^2 / 4s |\hat{\omega} + K|^4}. \qquad (16)$$

Reynolds stress

Reciprocal Prandtl number

$$\frac{\chi}{\mu_\perp} = \frac{\gamma|\hat{\omega} + K|^2}{|\hat{\omega}|^2 K},$$

$$\frac{\chi}{\mu_\parallel} = \frac{|\hat{\omega} + K|^2}{|\hat{\omega}|^2}.$$

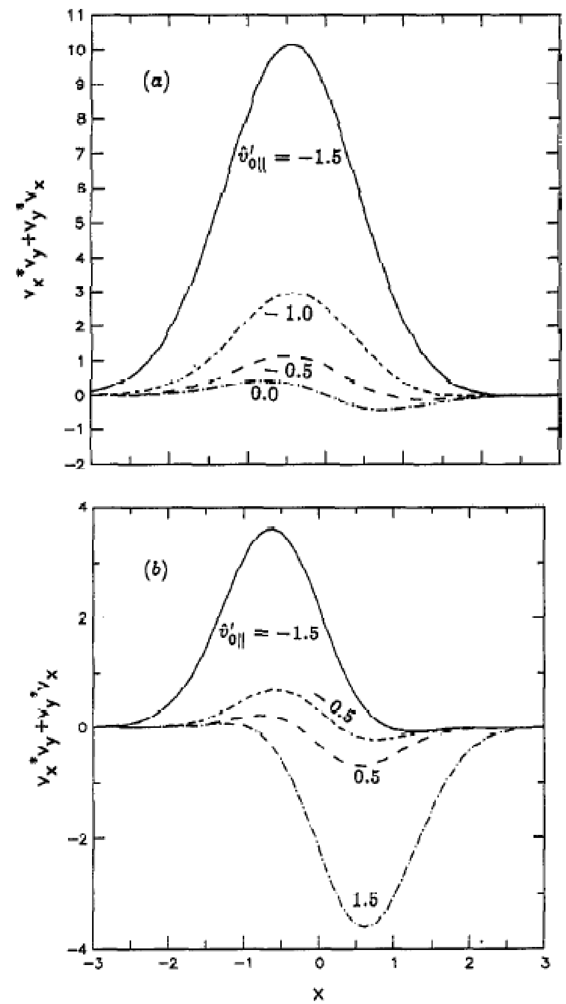

FIG. 2. Micro-Reynolds stress distribution π_{xy} around the mode rational surface $x=0$ for $\eta_i=1$, $\tau=1$, $b_s=0.1$ and (a) $s=0.1$, $\hat{v}'_{0\|} = -1.5$, -1.0, -0.5, and 0.0; (b) $s=0.5$, $\hat{v}'_{0\|} = -1.5$, -0.5, 0.5, and 1.5.

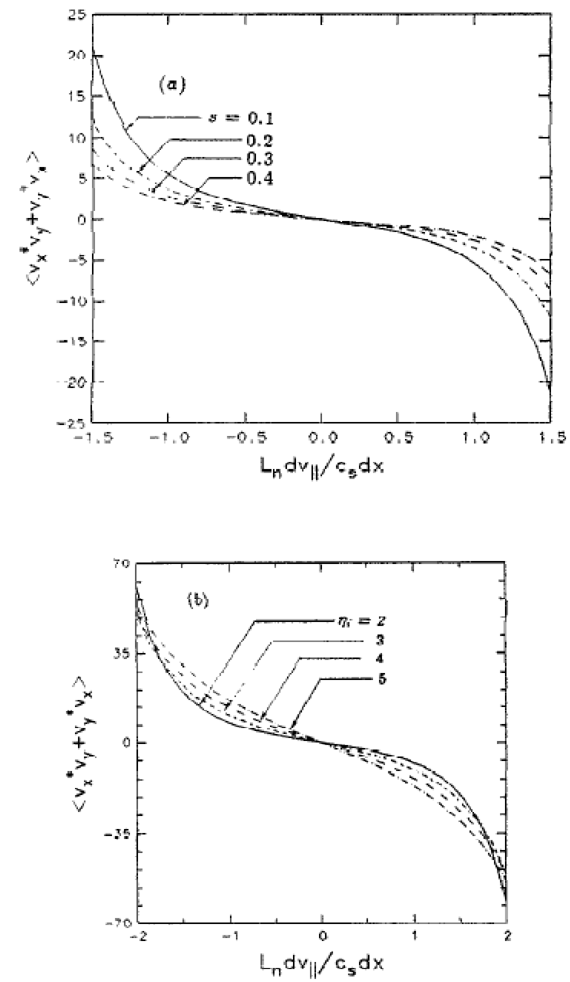

FIG. 3. Reynolds stress $\langle \pi_{xy} \rangle$ vs $\hat{v}'_{0\|} = L_n\, dv_\| / c_s\, dx$ for $b_s=0.1$, $\tau=1$, and (a) $\eta_i=1$, $s=0.1$, 0.2, 0.3, and 0.4; (b) $s=0.1$, $\eta_i=2$, 3, 4, and 5.

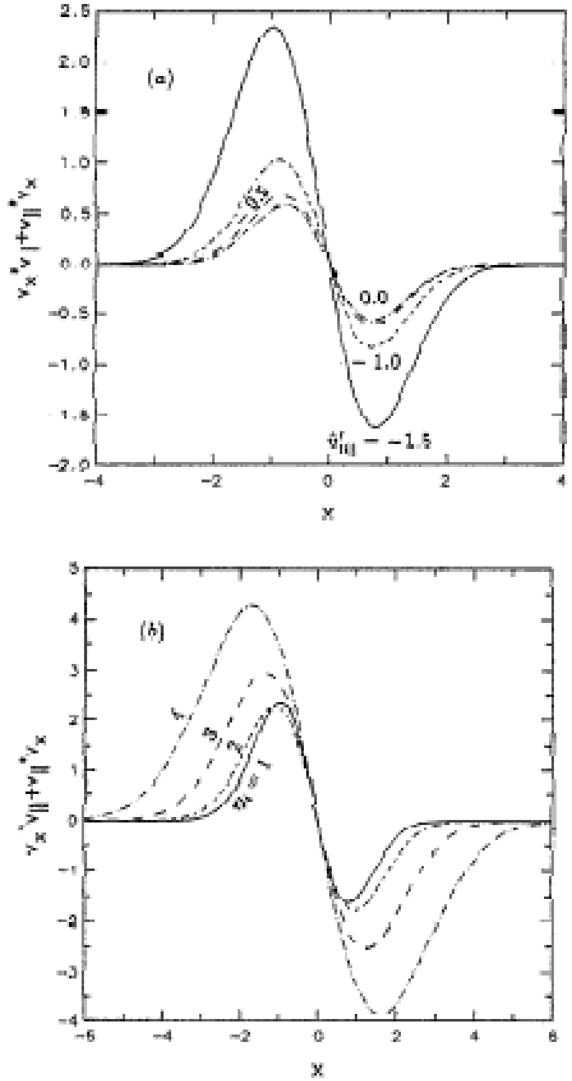

FIG. 4. Micro-Reynolds stress distribution $\pi_{x\parallel}$ around the mode rational surface $x=0$ for $\tau=1$, $b_s=0.1$, $s=0.1$ and (a) $\eta_i=1$, $\hat{v}'_{0\parallel} = -1.5, -1.0, -0.5$, and 0.0; (b) $\hat{v}'_{0\parallel} = -1.5$, $\eta_i=1$, 2, 3, and 4.

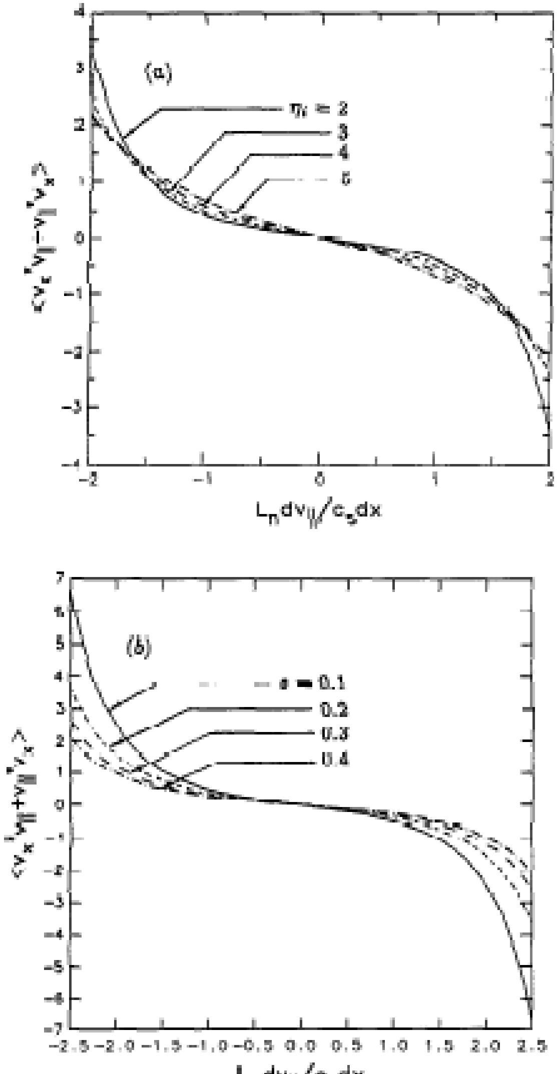

FIG. 5. Reynolds stress $\langle \pi_{x\parallel} \rangle$ vs $\hat{v}'_{0\parallel} = L_n\, dv_{\parallel}/c_s\, dx$ for $b_s=0.1$, $\tau=1$ (a) $s=0.1$, $\eta_i=2$, 3, 4, and 5; (b) $\eta_i=3$, $s=0.1$, 0.2, 0.3, and 0.4.

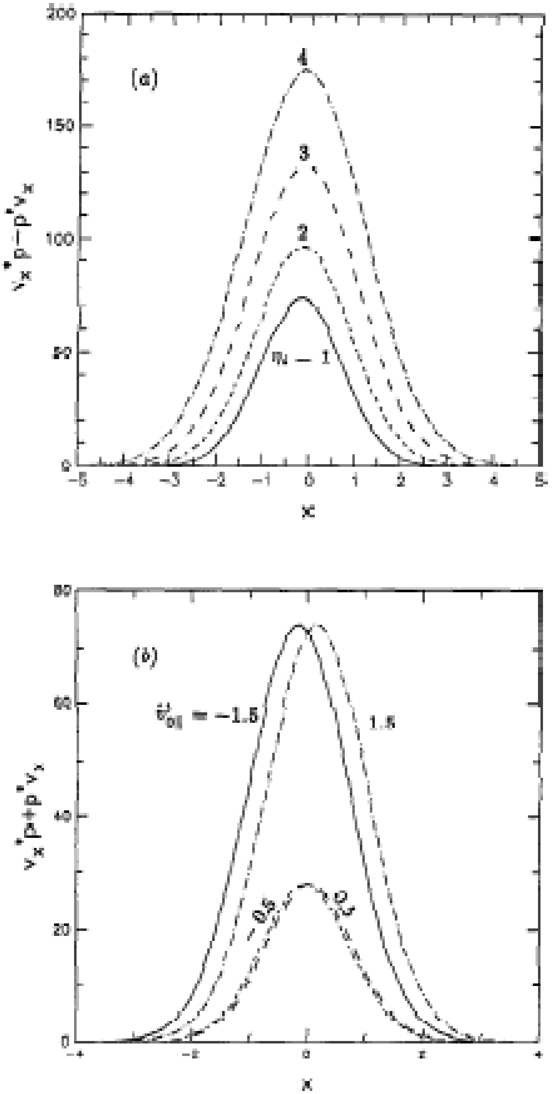

FIG. 6. Energy flux distribution q_x around the mode rational surface $x=0$ for $\tau=1$, $b_s=0.1$, $s=0.1$ and (a) $\hat{v}'_{0\parallel} = -1.5$, $\eta_i=1$, 2, 3, and 4; (b) $\eta_i=1$, $\hat{v}'_{0\parallel} = -1.5, -0.5, 0.5$, and 1.5.

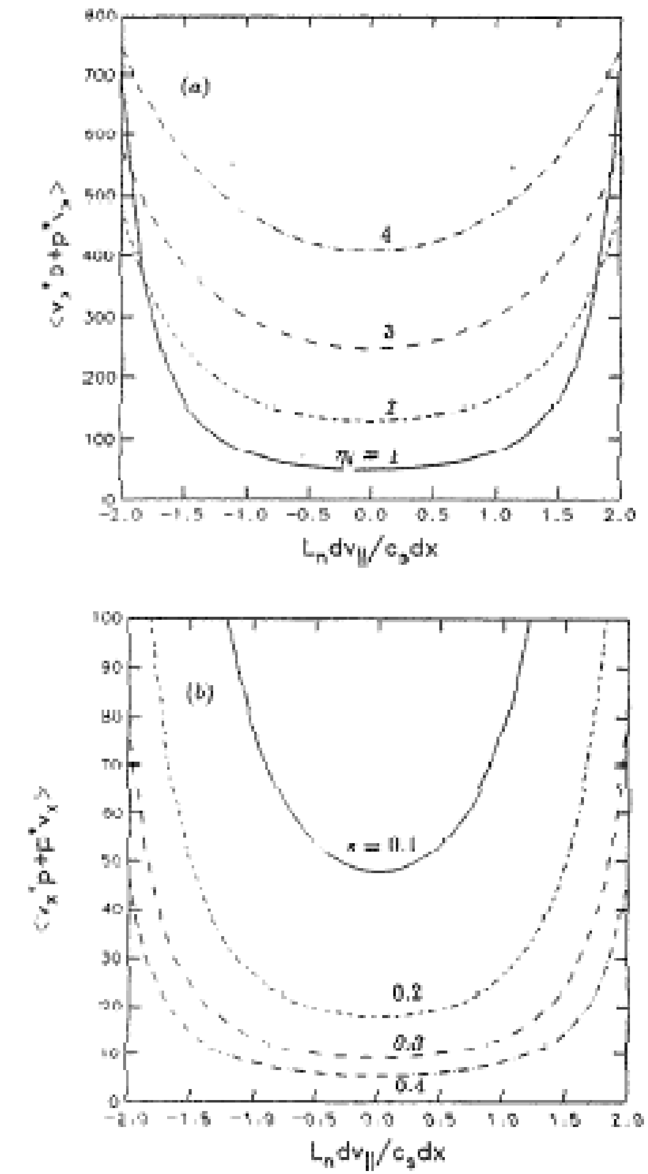

FIG. 7. Energy flux $\langle q_x \rangle$ vs $\hat{v}'_{0\|} = L_n\, dv_\|/c_s\, dx$ for $b_s=0.1$, $\tau=1$, and (a) $x=0.1$, $\eta_i=2$, 3, 4, and 5; (b) $\eta_i=1$, $x=0.1$, 0.2, 0.3, and 0.4.

The equation for generation of the poloidal velocity $\langle v_\theta \rangle$ is

$$\frac{\partial}{\partial t}\langle v_\theta\rangle = -\frac{1}{r}\frac{\partial}{\partial r}\left(r\langle \pi_{xy}\rangle\right). \tag{27}$$

Saturation amplitude

$$x\frac{dv_\|}{dx} \sim \tilde{v}_\|(x), \qquad \phi_0 \sim \frac{T_e}{e}\frac{\rho_s}{L_n}\hat{v}'_{0\|}.$$

$$\frac{\partial}{\partial x}\langle \pi_{xy}\rangle = -\frac{c^2T_e^2}{e^2L_n^3B^2}\frac{k_y\rho_s(\pi)^{1/2}}{s^{5/2}}\frac{\gamma^{1/2}|\hat{\omega}|^2K}{|\hat{\omega}+K|^2} \times\left(3+\frac{\gamma K^2\hat{v}_{0\|}'^2}{2s|\hat{\omega}+K|^4}\right)\hat{v}_{0\|}'^2\hat{v}''_{0\|}$$

$$= -\frac{c^2T_c^2}{e^2L_n^3B^2}H(\eta_i,\tau,s,b_s,\hat{v}'_{0\|},\hat{v}''_{0\|}), \tag{28}$$

where $\hat{v}''_{0\|} = L_n^2\, d^2v_\|/c_s\, dx^2$ and

$$H(\eta_i,\tau,s,b_s,\hat{v}'_{0\|},\hat{v}''_{0\|}) = \frac{k_y\rho_s(\pi)^{1/2}}{s^{5/2}}\frac{\gamma^{1/2}|\hat{\omega}|^2K}{|\hat{\omega}+K|^2} \times\left(3+\frac{\gamma K^2\hat{v}_{0\|}'^2}{2s|\hat{\omega}+K|^4}\right)\hat{v}_{0\|}'^2\hat{v}''_{0\|}.$$

$$\frac{\partial}{\partial t}\langle v_\theta\rangle = -\frac{1}{r}\frac{\partial}{\partial r}(r\langle\pi_{xy}\rangle) - \nu^{\mathrm{nc}}(\langle v_\theta\rangle - v_\theta^{\mathrm{nc}}), \qquad (29)$$

where v_θ^{nc} is the equilibrium poloidal velocity and

$$\nu^{\mathrm{nc}} = \frac{\nu_{ii}}{\epsilon^{3/2}(1+\nu_*)(1+\epsilon^{3/2}\nu_*)}, \qquad (30)$$

with $\nu_* = \nu_{ii} qR/v_{\mathrm{th}}\epsilon^{3/2}$ and ϵ is the inverse aspect ratio, q is the safety factor, R is the major radius, and ν_{ii} is the ion–ion collision frequency. In steady state, Eq. (29) reduces to

$$\langle v_\theta\rangle - v_\theta^{\mathrm{nc}} = -\frac{1}{\nu^{\mathrm{nc}}}\frac{\partial}{\partial x}\langle\pi_{xy}\rangle. \qquad (31)$$

For the dimensionless parameters $(\eta_i, s, \tau, \hat{v}'_{0\|}, b_s)$ of order unity, the poloidal acceleration from the divergence of the momentum flux is of the magnitude $(cT_e/eBL_n)^2/L_n \simeq v_{de}^2/L_n$, compared with the neoclassical damping rate ν^{nc}.

In order to make a further comparison, it is assumed that the equilibrium poloidal velocity v_θ^{nc} is negligible, and that the plasma is around the boundary between the Pfirsch–Schlüter and the plateau regimes with $l \sim qR$, so that $\nu^{\mathrm{nc}} \simeq \nu_{ii}$. Then the steady-state poloidal velocity [Eq. (31)] reduces to

$$\langle v_\theta\rangle = \frac{1}{\nu_{ii}}\frac{v_{de}^2}{L_n} H(\eta_i, \tau, s, b_s, \bar{v}'_{0\|}, \bar{v}''_{0\|}). \qquad (32)$$

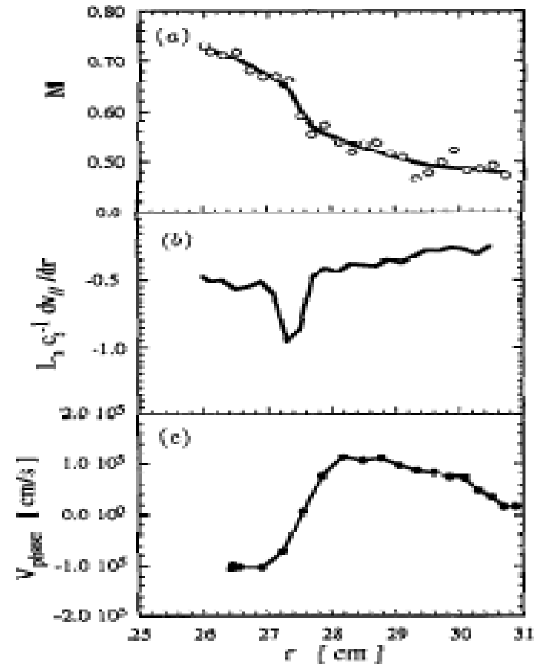

FIG. 10. The profile of (a) Mach number and (b) $\hat{v}'_{0\|} = L_n\, dv_\| / c_s\, dx$ measured at the plasma edge in the TEXT-U tokamak. (c) The poloidal velocity profile in a discharge of TEXT-U with $I_p = 160$ kA, $B_T = 2.2$ T, and $\bar{n}_e = 1.5\times 10^{13}$ cm^{-3}.

Home work：ITG turbulence induces energy transport but not momentum transport when parallel velosity shear is zero. Why?

Outline

1. Introduction
2. Instabilities
3. Turbulence and Zonal Flow
4. Transport
5. **Summary**

- **Tokamak plasma is a non-equilibrium many-body system where charged particles move under the action of electromagnetic field, that in return produces electromagnetic field (self-consistent field) and, therefore, influence the behavior of the system. It is a system of great freedom, fluent collective effects and motion modes. There are many unknown nonlinear physics processes (such as turbulence, chaos and self-organized order structures etc.)**
- **Gradient of plasma parameters (including magnetic field) drive a variety of micro-instabilities (ITG, ETG, TEM, and AITG etc.) and turbulence.**
- **Turbulence induces anomalous (turbulent) mass, momentum and energy across field transport.**
- **Turbulence also generates zonal flows which reduces the turbulent transport and improves confinement.**
- **Great progress has been achieved but we still face many challenges in this field which has a prosperous prospect.**

Thank you for your attention!